ORGANOMETALLICS

ARTICLE

pubs.acs.org/Organometallics

Synthesis of Imino-Enamido Hafnium and Zirconium Complexes: A New Family of Olefin Polymerization Catalysts with Ultrahigh-Molecular-Weight Capabilities

Ruth Figueroa, Robert D. Froese, Yiyong He, Jerzy Klosin,* and Curt N. Theriault

Corporate R&D, The Dow Chemical Company, 1776 Building, Midland, Michigan 48674, United States

Khalil A. Abboud

Department of Chemistry, University of Florida, Gainesville, Florida 32611, United States

Supporting Information

ABSTRACT: Bidentate, nitrogen-containing molecules are of interest as ligands in transition-metal-catalyzed olefin polymerization. A computational evaluation of a series of 1,2-bis-imines, 1,2-imine-enamines, and 1,2-bis-enamines of cyclic and acyclic derivatives was conducted to understand the relative thermodynamic stabilities of these compounds. The five- and six-membered-ring 1,2-imine-enamines were found to be more stable than the other tautomers, while the 1,2-bis-imines were calculated to have the lowest energy among four- and seven-membered-ring and acyclic derivatives. On the basis of the computational results, literature examples, and prior experience with imino-amido catalysts, 1,2-imine-enamines containing a cyclohex-2-enylidene backbone were targeted as ligands for a new family of polyolefin catalysts. The desired ligands were prepared in three steps, starting from the commercially available 1,2-cyclohexanedione, and subsequently converted into hafnium and zirconium complexes. An ethylene/1-octene copolymerization study conducted at 120 °C demonstrated that the hafnium complex possessed very good activity for the production of polymers with ultrahigh molecular weight (M_w of 1037 kDa) and moderate 1-octene incorporation. This molecular weight is 20 times higher than that produced by the titanium constrained geometry catalyst (CGC) under the same polymerization conditions. The imino-enamido zirconium complex exhibited slightly lower activity than that observed for the hafnium catalyst, yielding an ethylene/1-octene copolymer with M_w and mol % 1-octene incorporation of 509 kDa and 6.4, respectively. The polymerization reactions with these catalysts conducted in the presence of diethylzinc led to a sharp decrease in the observed polymer molecular weights, indicative of effective chain transfer. These imino-enamido complexes exhibit higher activity, produce higher molecular weight polymers, incorporate higher levels of 1-octene, and demonstrate significantly improved thermal stability relative to analogous imino-amido complexes reported previously.

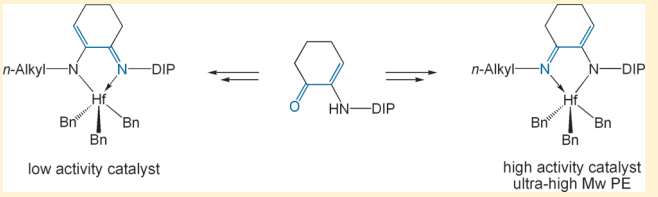

INTRODUCTION

There has been continued research aimed at the discovery of new olefin polymerization catalysts[1] that would allow for either the production of new polyolefin products[2] or lead to significant improvements to current polymerization processes.[3] Some important characteristics of olefin polymerization catalysts for the synthesis of polyolefin copolymers, specifically poly(ethylene-co-α-olefin), include molecular weight capabilities, reactivity toward α-olefins, catalytic activity, and reactivity toward chain transfer agents such as hydrogen and alkylaluminum or -zinc compounds. Equally important is how these characteristics are influenced by reaction conditions, such as concentration of monomers and temperature.

Recently, we[4−6] and others[7] have reported the use of group 4 imino-amido complexes, a class of compounds originally introduced by Union Carbide Corp., as precatalysts for olefin polymerization reactions.[8] Imino-amido complexes are attractive, as they are readily prepared from commonly available starting materials and a large and diverse library of such complexes is accessible. More importantly, they exhibit good catalytic activities at industrially relevant temperatures (greater than 100 °C), are capable of producing very high molecular weight ethylene-based copolymers, and have the ability to undergo reversible chain transfer with diethylzinc to produce olefin block copolymers.[5] A few representative imino-amido complexes investigated in our laboratory are displayed in Scheme 1.

Despite the advantages of imino-amido precatalysts, their industrial utility might be limited due to the thermal instability of these materials. For example, precatalysts such as **1** were found to decompose at elevated temperature to form ene-diamido

Received: December 28, 2010
Published: March 11, 2011

Scheme 1. Examples of Previously Studied Imino−Amido Complexes[a]

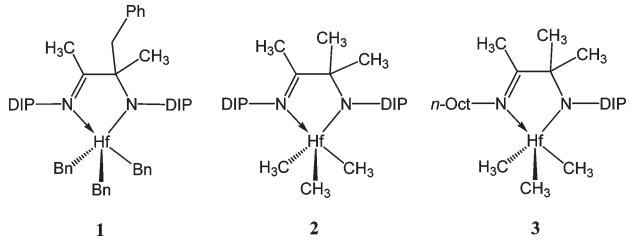

[a] DIP = 2,6-*i*-$Pr_2C_6H_3$, Bn = CH_2Ph.

Scheme 2. Structural Rearrangement of Imino−Amido Complexes 1 and 5a

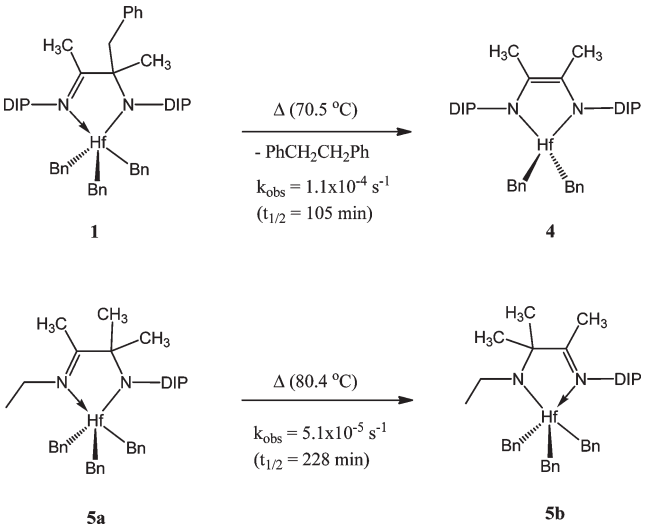

complexes (**4**) via dibenzyl elimination (Scheme 2).[4] The rate of decomposition was found to be dependent on the nature of the metal, with faster rates observed for zirconium derivatives than for hafnium analogues. A second subclass of imino-amido complexes containing the trimethylethylidene ligand bridge (e.g., **3**, **5a**) also was found to be thermally unstable, decomposing via a 1,2-methyl backbone rearrangement. This reaction results in the production of a more stable isomeric precatalyst **5b** (Scheme 2), but one that exhibits poorer polymerization performance.[6] We desired to prepare imino-amido complexes with a ligand framework resistant to the aforementioned deactivation pathways while maintaining polymerization attributes of the best examples from this family of catalysts.

Over a decade ago, van Asselt and co-workers[9] described the reaction of 1,2-cyclohexanedione (**6**) with excess isopropylamine to yield imino-enamine **7**, rather than the expected bis-imine **8** product (Scheme 3). Subsequently, groups from Mitsui Petrochemical Industries[10] and DuPont[11] reported the analogous reaction between 1,2-cyclohexanedione and 2 equiv of 2,6-diisopropylaniline to form imino-enamine **9** (Scheme 3). Again, formation of the bis-imine isomer was not observed. Other imino-enamines with the cyclohex-2-enylidene backbone containing alkyl substituents on the nitrogen atoms have been also reported.[12,13]

Scheme 3. Synthesis of Imino−Enamines 7 and 9

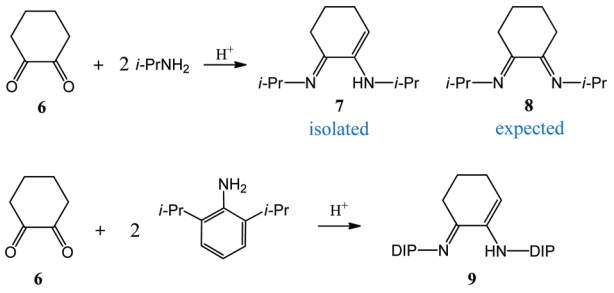

These imino-enamines attracted our interest because they are structurally similar to the imino-amine ligands and contain the cyclohex-2-enylidene backbone which, in principle, should yield configurationally stable complexes. Ligand **9** has been used in the preparation of nickel,[10,11] palladium,[14] and aluminum compounds[15] but had not been yet reported in the synthesis of group 4 transition metal complexes.[16] Neutral and cationic nickel complexes with acyclic imino-enamido ligands were reported as well.[17] Herein, we report a study of the computational stability of various 1,2-bis-imines, 1,2-imino-enamines, and 1,2-bis-enamines and the preparation of hafnium and zirconium complexes containing imino-enamido ligands with a cyclohex-2-enylidene backbone and their olefin polymerization characteristics.[18]

RESULTS AND DISCUSSION

Computational Study of Bis-Imines vs Imino-Enamines. It is not intuitively obvious why the reaction between primary amines and acyclic 1,2-diones leads to the formation of 1,2-bis-imines, whereas the analogous reaction with 1,2-cyclohexanedione produces the 1,2-imino-enamine isomer, as described above. It was also reported[13] that the reaction of isopropylamine with cycloheptane-1,2-dione gives the corresponding bis-imine, whereas the reaction of the same amine with 1,2-cyclohexanedione leads to the imino-enamine. These observations clearly indicate that there are subtle thermodynamic preferences that exist between such 1,2-bis-imines and 1,2-imino-enamines. To understand the factors that control these preferences and to help us determine which elements are critical to produce stable imine-enamines suitable for complexation with early transition metals, a computational study was carried out on the molecules shown in Scheme 4. Ground-state energies for alkyl (*i*-Pr)- and aryl-based (DIP) bis-imines (trans/trans (a), trans/cis (b), and cis/cis (c) isomers), imino-enamines (d), and bis-enamines (e) were calculated using density functional theory (DFT) and G3MP2B3 methods[19,20] for the four-, five-, six-, and seven-membered-ring and acyclic derivatives (Scheme 4). These data indicate that the nitrogen substitution (alkyl vs aryl) only has a minor effect on the relative energies in each series. For this reason, the following discussion will include only the data for the *i*-Pr derivatives calculated using the high-level G3MP2B3 method.

There is a clear effect of the bridging unit on the relative stability of 1,2-bis-imines and 1,2-imine-enamines. For five- and six-membered-ring derivatives, the imino-enamine tautomers (**11d**, **7**) are favored considerably. Within five-membered-ring derivatives, the imino-enamine isomer **11d** is lowest in energy and is favored over the next lowest trans/cis bis-imine **11b** by 5.9

Scheme 4. Calculated Ground-State Energy Differences between Various Isomers[a]

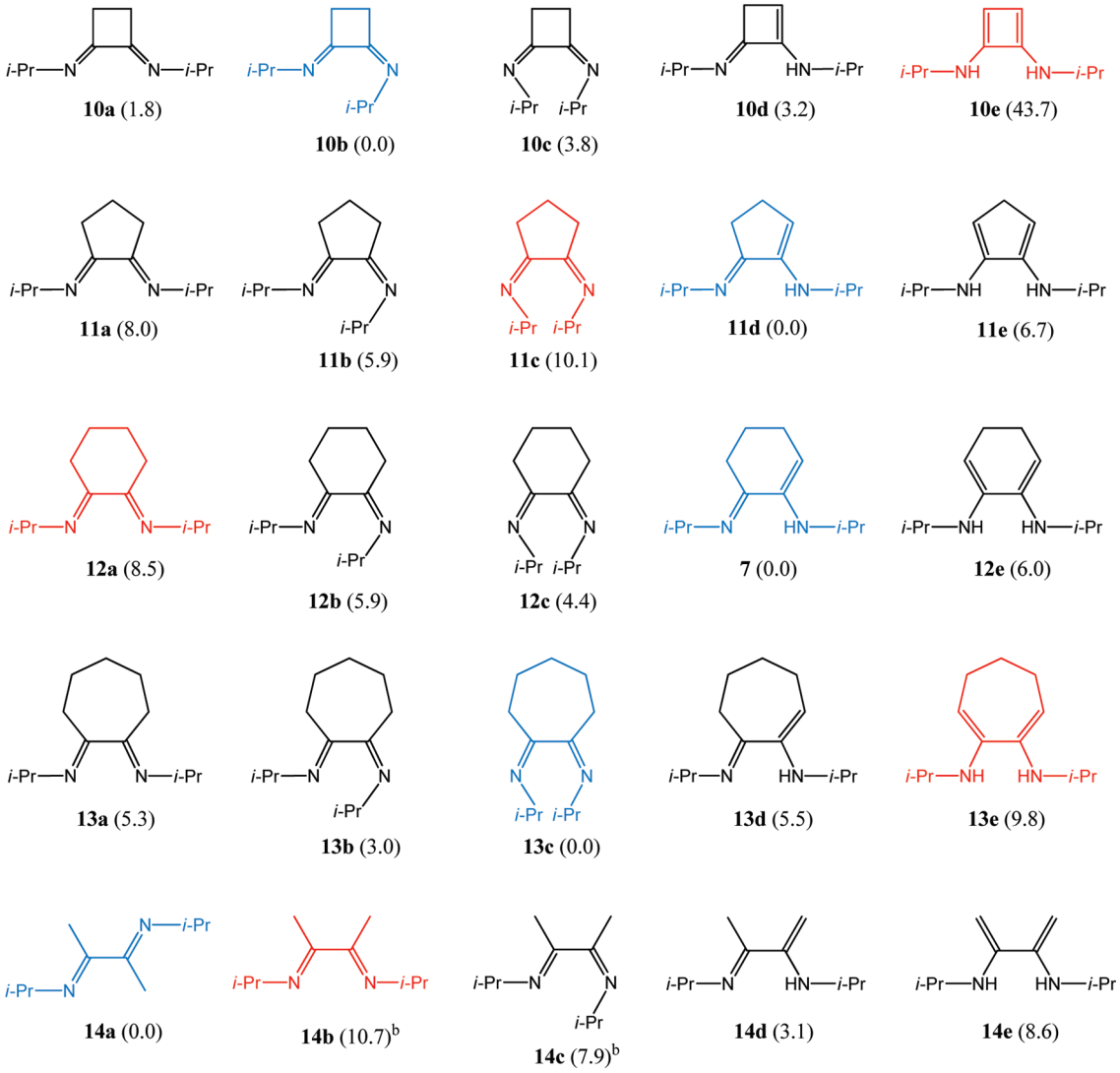

[a] Calculations were performed using the G3MP2B3 method. Relative enthalpies are in kcal/mol. Structures in blue and red correspond to the lowest and highest energy compounds within each series. [b] Optimized with the N=C−C=N fragment constrained in a coplanar σ-cis configuration.

kcal/mol. Within six-membered-ring compounds, the imino-enamine **7** is favored over the cis/cis bis-imine **12c** by 4.4 kcal/mol. Five and six-membered-ring trans/trans bis-imines **11a** and **12a** are higher in energy than the corresponding imino-enamine by 8.0 and 8.5 kcal/mol, respectively.[21] Interestingly, within the seven-membered-ring compounds, the relative stability of bis-imine and imino-enamine is reversed, with the bis-imine tautomer **13c** being lower in energy by 5.5 kcal/mol. For the four-membered-ring series, the bis-imine **10b** is preferred over imine-enamine **10d** by 3.2 kcal/mol. In all cases, bis-enamine isomers are higher in energy compared to imine-enamines, with the largest difference calculated for the four-membered-ring analogue **10e** due to the formation of the antiaromatic structure.

There are a few important factors that determine the relative stability of isomers shown in Scheme 4. For the following discussion, it is important to point out that cyclic mono-imines are more stable than the corresponding enamines by a few kcal/mol.[22] This trend is opposite to that observed for hydrocarbon analogues, where 1-methylcycloalkenes are more stable than the corresponding methylenecycloalkanes by at least 2 kcal/mol.[23] Two factors appear critical for the relative stability of trans/trans bis-imine and imino-enamine tautomers, and both are related to the relative arrangement of the N−C−C−N fragment. One of those factors is the hydrogen bonding between the imine nitrogen and enamine NH group, which would be expected to be strongest for the five- and six-membered-ring derivatives, due to the close proximity of these groups resulting from the nearly coplanar arrangement of the N−C−C−NH fragment. The N=C−C−NH torsion angles in the five-, six- and seven-membered-ring imino-enamines are approximately 4, 5, and 44°, respectively. For the six-membered-ring imine-enamine **9**, this torsion angle was determined crystallographically to be 3.7° (vide infra). The hydrogen bond, however, would not be expected to be stronger than 3−6 kcal/mol in compounds of this type,[24] which is still less than the energy difference between the trans/trans bis-imine and imino-enamine tautomers for the five- and six-membered-ring derivatives. Thus, hydrogen

dx.doi.org/10.1021/om101207a |*Organometallics* 2011, 30, 1695–1709

bonding cannot be the sole contributing factor to the stability of the five- and six-membered-ring imino-enamines.

A second major contributor to the enhanced stability of five- and six-membered-ring imino-enamines over the corresponding trans/trans bis-imines is the destabilization of the latter caused by repulsion between the lone-pair electrons of the bis-imine nitrogen atoms. Bis-imine destabilization should be the strongest for five- and six-membered-ring derivatives due to the close proximity of two imine nitrogen atoms, reduced in the four-membered system as the nitrogen atoms are further apart and the angle directs the lone pairs somewhat away from each other, reduced also in the seven-membered-ring system where the ring twist allows the lone pairs to avoid one another, and nonexistent in the acyclic derivative which assumes a σ-trans configuration. The N═C−C═N torsion angles in the five-, six-, and seven-membered-ring trans/trans bis-imines are approximately 0, 46, and 91°, respectively. Thus, the five- and six-membered-ring trans/trans bis-imines are disfavored due to lone-pair−lone-pair repulsions and imine-enamines are favored due to stronger hydrogen bonding. Consistent with the bis-imine destabilization hypothesis is that cyclic mono-imines are more stable than their enamine counterparts.[21] Another piece of supporting information that the lone-pair−lone-pair interaction is a destabilizing feature is that the five- and six-membered-ring bis-imines generally do not exist in the trans/trans form unless large steric groups such as DIP reside on the imine nitrogen atoms.[25] For example, trans/cis bis-imines **11b** and **12b** are more stable than their trans/trans counterparts **11a** and **12a** by 2.1 and 2.6 kcal/mol, respectively.[26,27] Additionally, for acyclic bis-imines, the σ-trans isomer **14a** is lower in energy than the σ-cis rotamer **14b** by ca. 10 kcal/mol. Another piece of intriguing evidence comes from the Cambridge Crystallographic Database, where acyclic bis-imines were examined. All acyclic 1,2-bis-imines were found to exist in the σ-trans conformation,[25b,28] except for three,[29] which contain CF_3 groups in the 2- and 3-positions of the 1,4-diazabutadiene fragment. In the σ-trans configuration, the lone pairs of the fluoride atoms appear capable of having a strong repulsive interaction with the imine lone pair, leading to considerable rotation of the two imine fragments away from each other, as observed experimentally (N═C−C═N torsion angle between 55 and 64°).[29]

Six- and seven-membered-ring bis-imines are intriguing in that the cis/cis isomers are lower in energy than their trans/trans and trans/cis counterparts. Since only one of the imines needs to adopt the cis configuration to avoid the lone-pair−lone-pair interaction, it is surprising that both bis-imines adopt the cis/cis configuration. However, the severely twisted N═C−C═N fragment allows for the reduction of steric interaction between the two *i*-Pr groups. The seven-membered-ring cis/cis bis-imine **13c** has the lowest ground-state energy among all seven-membered-ring derivatives. Published ^{1}H and ^{13}C NMR data[13] for the seven-membered-ring bis-imine are most consistent with the C_2-symmetric (chiral) structure **13c**.[30] Within the four-membered-ring series, the trans/cis bis-imine **10b** has the lowest energy, with the trans/trans isomer **10a** being 1.8 kcal/mol higher in energy.

The relative energy trends shown in Scheme 4 are comparable to energy differences calculated for the cyclic 1,2-keto-enamine/1,2-keto-imine and 1,2-keto-enol/1,2-diketone pairs, pointing to a common reason for the observed stability trends.[31]

The most significant result from this computational study is that the five- and six-membered-ring imino-enamines are considerably lower in energy than any other derivative in the five- and six-membered-ring series. This indicates that these two imino-enamines should exist exclusively as a single isomer and thus be good candidates for complexation with early-transition-metal precursors.

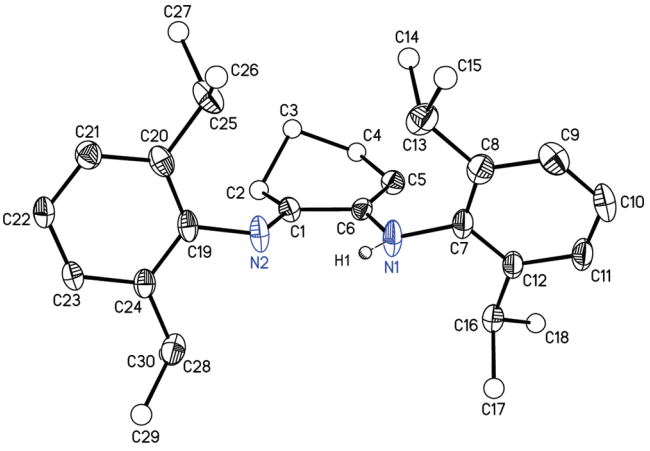

Figure 1. Molecular structure of **9**. Hydrogen atoms, except H1, are omitted for clarity. Thermal ellipsoids are shown at the 40% probability level. Atoms refined isotropically are represented by open spheres. Selected bond lengths (Å) and angle (deg): C1−N2 = 1.306(2), C6−N1 = 1.352(2), C5−C6 = 1.390(2), N1−H1 = 0.85(3), N2−H1 = 2.175; N1−H1−N2 = 111.5.

Scheme 5. Synthesis of Hafnium Complex 15

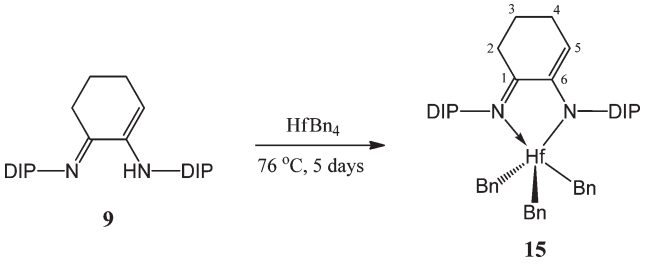

Synthesis of Ligands and Complexes. It was of interest to us to prepare hafnium and zirconium complexes containing cyclohex-2-enylidene-bridged imino-enamido ligands, direct analogues of the imino-amido complexes **2** and **3**, and evaluate their olefin polymerization characteristics. Since ligand **9** is readily accessible, preparation of its hafnium complex was undertaken initially to compare properties of this precatalyst with those of the imino-amido analogue **2**. The desired ligand, (*E*)-*N*-(2-((2,6-diisopropylphenyl)amino)cyclohex-2-enylidene)-2,6-diisopropylbenzenamine (**9**), was prepared in 50% yield by following a literature procedure.[11b] Single-crystal X-ray analysis of **9** confirms the planar arrangement of the N═C−C═NH fragment (Figure 1). The reaction of **9** with $Hf(CH_2Ph)_4$ in toluene produced, after 5 days at 76 °C, the desired complex **15** in about 90% yield by NMR (Scheme 5). Complex **15** was obtained in pure form in 53% yield after crystallization from toluene/hexane. The NMR spectra of **15** are consistent with C_s symmetry in solution. Resonances of interest observed in the ^{1}H NMR spectrum[32] of **15** include two septets appearing at 2.74 and 3.51 ppm, which are assigned to the *i*-Pr methine protons of the 2,6-diisopropylphenyl groups of the imine and enamine nitrogen substituents, respectively. These assignments were confirmed by

Scheme 6. General Strategy for the Synthesis of Unsymmetrical Imino-Enamines

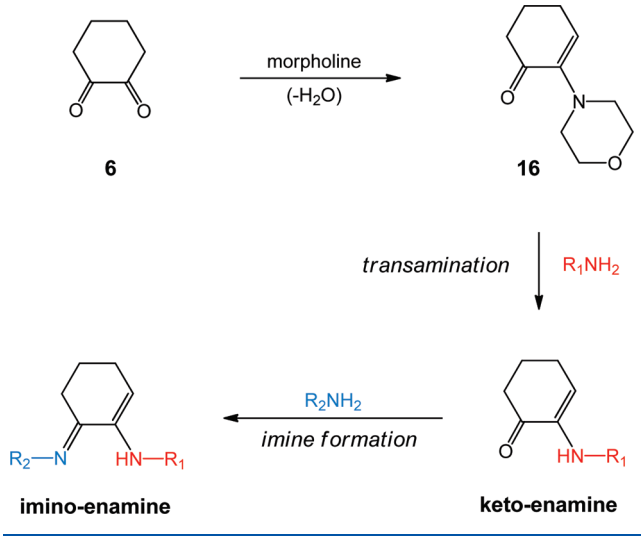

1D NOESY measurements.[32] Irradiation of the vinyl proton H5 resonating at 4.96 ppm shows a strong NOE of the *i*-Pr methine at 3.51 ppm, the *i*-Pr methyl groups at 1.14 ppm, and the cyclohex-2-enylidene allylic protons resonating at 1.81 ppm. All benzyl methylene protons appear as a singlet at 2.10 ppm, indicating fast exchange of all three benzyl groups on the NMR time scale. In addition to NMR and elemental analysis, complex **15** was also characterized by X-ray single crystal analysis (vide infra).

Due to the higher polymerization activity of imino-amido complex **3** relative to that of **2**, preparation of an imino-enamine complex analogous to **3** was highly desired. Preparation of imino-enamine ligands with two different substituents at the imine and enamine nitrogen atoms requires a different synthetic approach, as both groups need to be introduced sequentially. The general strategy for the preparation of such unsymmetrical imino-enamine ligands is outlined in Scheme 6 and involves preparation of keto-enamine via transamination of morpholino-ketone **16** with a primary amine to give a keto-enamine with the desired R_1 group, followed by condensation of the product with another 1 equiv of primary amine to form the desired imino-enamines.

The synthesis was initiated with the preparation of the morpholine derivative **16**, which was synthesized in 95% yield via condensation of 1,2-cyclohexanedione with morpholine (Scheme 6).[33] Compound **16** was fully characterized by both NMR spectroscopy and single-crystal X-ray analysis.[34] Transamination of enamine **16** using *p*-toluenesulfonic acid hydrate (PTSA) was used previously to form aryl-based keto-enamines.[35] Transamination of **16** under similar reaction conditions to those previously reported[35b] with 1 equiv of 2,6-diisopropylaniline and 0.1 equiv of acid at 50 °C resulted in a poor yield of 2-((2,6-diisopropylphenyl)amino)cyclohex-2-enone (**17**) after 24 h. Alternatively, we found that when the reaction was conducted at 80 °C using 1.0 equiv of PTSA, **17** can be isolated in high yield as a yellow solid. The transamination route is necessary to obtain clean product **17**, as direct condensation of **6** with 1 equiv of 2,6-diisopropylaniline gives a mixture of products. The ^{1}H NMR spectrum of **17** shows the presence of a triplet at 4.95 ppm, indicating that the compound exists as the keto-enamine rather than the keto-imine. The keto-enamine form of **17** is maintained also in the solid state, as shown by single-crystal X-ray analysis.[34] DFT calculations indicate that keto-enamine **17** is 7.9 kcal/mol more stable than the isomeric keto-imine. This energy difference is similar to that calculated for the six-membered-ring imino-enamine **9** and its bis-imine tautomer. The presence of only one doublet for the *i*-Pr methyl groups at 1.10 ppm is indicative of rapid rotation of the 2,6-diisopropylphenyl fragment on the NMR time scale. To access the desired ligand, several different conditions were evaluated for the imine formation step. The best conversion was obtained when **7** was reacted with 1.0 equiv of *n*-octylamine and 1.0 equiv of formic acid. The product was isolated in 59.5% yield by column chromatography using silica buffered with triethylamine. However, the structure of the isolated imino-enamine (**18b**) was different from that of the desired ligand (**18a**), as shown by NOE analysis. Irradiation of the triplet at 5.04 ppm (^3J = 4.6 Hz) corresponding to the vinyl proton (H2) resulted in a strong NOE of a quartet (^3J = 7.0 Hz) at 2.91 ppm corresponding to the methylene protons H7 and no detectable NOE enhancement of the *i*-Pr groups. Additionally, irradiation of the pseudotriplet at 2.06 ppm assigned to the H5 methylene (assignment based on 1D TOCSY and COSY) showed strong enhancement to the resonances of the *i*-Pr groups. These measurements clearly indicate that the structure of the obtained ligand is that of **18b** instead of the desired **18a**. Interestingly, the ^{1}H NMR spectrum shows two doublets for the *i*-Pr methyl groups, indicating restricted rotation of the 2,6-diisopropylphenyl fragment on the NMR time scale. Reaction of **18b** with $Hf(CH_2Ph)_4$ quantitatively yielded **19** within 1 h at ambient temperature (Scheme 7). Complex **19** crystallized slowly from a hexane solution at −35 °C over a period of 2 weeks. In addition to 1D and 2D NMR spectroscopy, complex **19** was characterized by elemental analysis and single-crystal X-ray analysis (vide infra). The NOE experiments and X-ray analysis of **19** validated that the configuration of the imino-enamido fragment in this complex is the same as in the corresponding ligand **18b**.

The most likely reason for the observed outcome of the imine-formation reaction to produce **18b** is that the condensation reaction gives the desired ligand **18a**, which under acidic conditions isomerizes to the thermodynamically more stable **18b**. This is consistent with DFT calculations, which confirmed that **18b** is more stable than the desired ligand **18a** by 1.9 kcal/mol. This result suggests that perhaps this isomerization can be slowed down or eliminated if the imine-formation step is conducted under acid-free conditions. We turned our attention to titanium-induced imine formation reactions,[36] as this method does not involve acidic reaction conditions. Imine and enamine formation reactions were reported using both $TiCl_4$[36a−d] or premade titanium amido[36e] reagents.

Due to the high solubility of the *n*-octyl Hf complex **19**, the preparation of ligands with the shorter *n*-butyl chain on the imine nitrogen was considered to decrease solubility. The titanium reagent was prepared by refluxing $Ti(NMe_2)_4$ with 6 equiv of *n*-butylamine in toluene for 6 h under a constant nitrogen sweep to remove dimethylamine. Removal of the solvent gave the Ti-imido reagent as a brown-red glossy solid. The structure of the product is polymeric in nature ($(Ti(N\text{-}n\text{-}Bu)_2)_n$), as suggested by the broad features in the ^{1}H NMR spectrum[32] and results described previously by Bradley and Torrible.[37]

The reaction of **17** with the Ti-imido reagent at room temperature in toluene led to the formation of the desired product **20a** in good yield (Scheme 8). However, this reaction took about 2 days

Scheme 7. Synthesis of Hafnium Complex 19

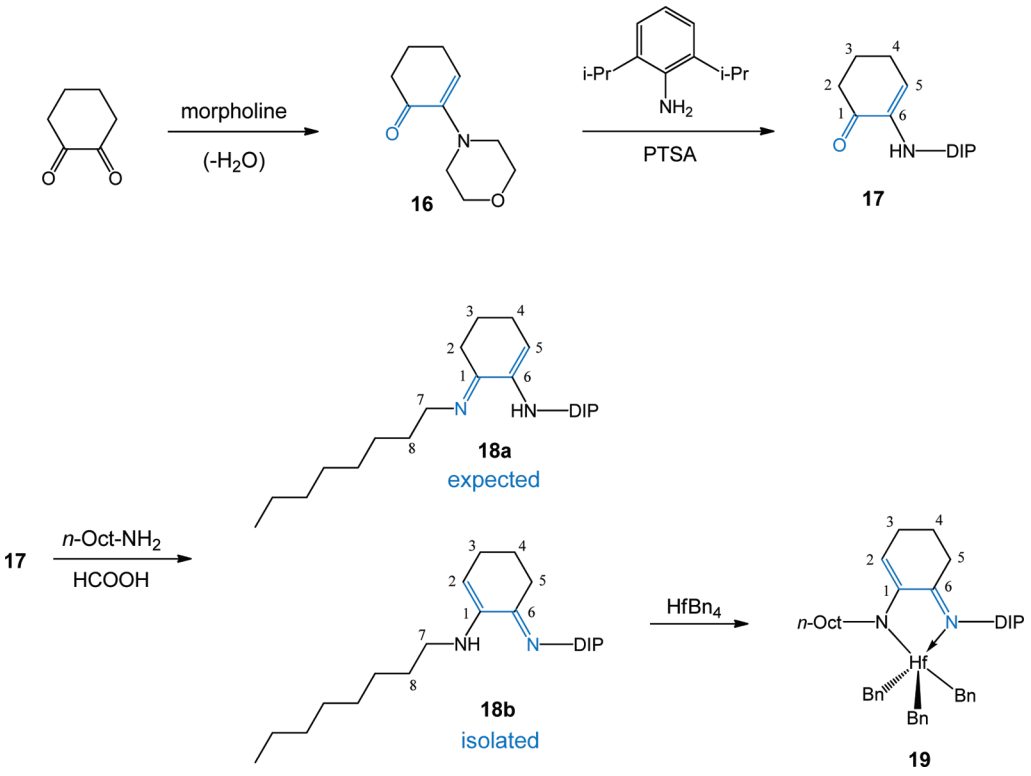

Scheme 8. Synthesis of Hafnium and Zirconium Complexes 21 and 22

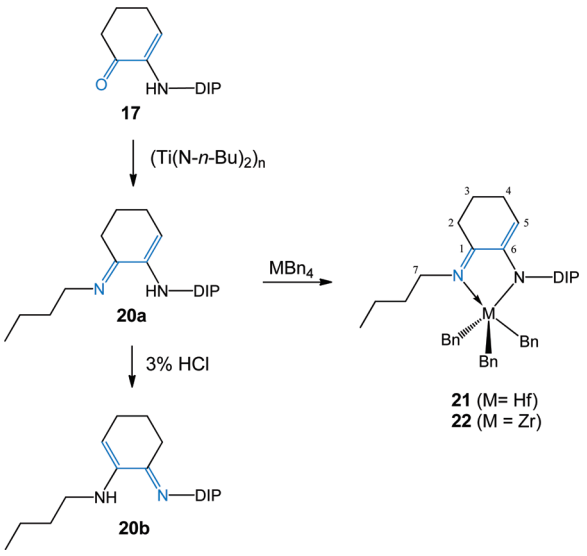

to reach full completion. It is important to maintain good stirring, which is made difficult by the formation of a thick brown byproduct during the course of the reaction. Despite the long reaction times, this synthetic method was found to be reliable and allowed preparation of this ligand on a multigram scale. The NMR spectra, including 1D NOESY data, are consistent with the desired structure **20a**. For example, irradiation of the triplet at 4.78 ppm (^3J = 4.6 Hz) corresponding to the vinyl proton H5 leads to a strong NOE of the septet at 3.39 ppm corresponding to *i*-Pr methine protons and a quartet at 1.96 ppm assigned to the methylene protons H4 and no detectable NOE enhancement of methylene protons H7. Unlike the case of **18b**, there is only one doublet present in the ^{1}H NMR spectrum of **20a** corresponding to the *i*-Pr methyl groups. The $^{13}C\{^1H\}$ NMR spectrum features a broad signal at 24.23 ppm ($\Delta\nu_{1/2}$ = 160 Hz) corresponding to the *i*-Pr methyl groups. This broad signal is an indication of hindered rotation about the 2,6-diisopropylphenyl fragment along the N−C(ipso) bond. The presence of only one doublet in the ^{1}H spectrum for the *i*-Pr methyl groups is most likely due to small chemical shift differences (smaller than in the case of the analogous resonances observed in the $^{13}C\{^1H\}$ spectrum) between the *i*-Pr methyl groups in the ^{1}H spectrum at the low-exchange regime. This leads to coalescence at temperatures lower than in the case of resonances in the $^{13}C\{^1H\}$ spectrum.

To test if ligand **20a** is stable to isomerization under neutral conditions, it was heated to 71 °C for 39 h in C_6D_6. ^{1}H NMR showed no indication of isomerization. On the other hand, addition of 3% HCl (in diethyl ether) relative to **20a**, dissolved in C_6D_6, led to complete and clean isomerization to produce **20b** within 10 min at ambient temperature. These experiments clearly indicate that these alkyl-imino-aryl-enamines are thermally stable but can be converted readily to thermodynamically more stable aryl-imino-alkyl-enamine isomers in the presence of a catalytic amount of acid.

Reaction of ligand **20a** with $M(CH_2Ph)_4$ (M = Hf, Zr) leads to clean formation of the desired complexes **21** and **22** in good yields at ambient temperature within 1 h (Scheme 8). No isomerization of the ligand framework was observed during

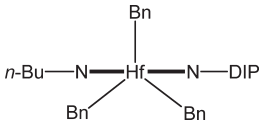

Figure 2. Schematic representation of possible low-temperature solution structure of **21**.

preparation of **21** and **22**, as confirmed by NOE experiments and X-ray crystallography. Both complexes exhibit C_s symmetry in solution, as shown by NMR spectroscopy. For example, the ^{1}H NMR spectrum of **21** shows only one *i*-Pr methine signal at 3.24 ppm and two doublets at 1.11 and 1.31 ppm corresponding to the *i*-Pr methyl groups, indicating that both *i*-Pr groups have the same chemical environment. The appearance of two separate resonances for the *i*-Pr methyl groups is due to the hindered rotation of the 2,6-diisopropylphenyl fragment along the N−C(ipso) bond, which leads to a different chemical environment of the methyl groups pointed toward and away from the cyclohex-2-enylidene bridge. This is a very common phenomenon in complexes containing the bulky 2,6-diisopropylphenyl fragment.[6,38] NOE experiments indicate that the upfield doublet (1.11 ppm) corresponds to the methyl groups pointing toward the bridge of the ligand. As hoped, both complexes are highly crystalline compared to **19** and can be crystallized easily from a toluene/hexane solvent mixture. In addition to other NMR techniques, all new ligands and complexes were studied by 1D TOCSY, which allows for unequivocal identification of protons associated with the two separate spin systems of cyclohex-2-enylidene and *N*-*n*-alkyl fragments. For example, irradiation of the methylene protons α to the N(imine) atom at 2.80 ppm in **21** clearly identified the remaining protons of the butyl chain resonances at 1.17, 1.06, and 0.77 ppm. The ^{1}H NMR spectrum of **21** contains a broad singlet at 2.11 ppm assigned to the three benzyl methylene groups. The broadness of this resonance indicates that the rate of chemical exchange of the three benzyl groups is reduced from a fast chemical exchange regime and suggested the possibility of freezing out this fluxional process at low temperature. When a solution of **21** in toluene-d_8 is cooled to −70 °C, three separate resonances for the benzyl groups are observed. The variable-temperature NMR spectra show coalescence of all three benzyl resonances at around −20 °C.[32] The most likely mechanism of this fluxional process is the rotation of the imino-enamido ligand about a C_3 axis of the $HfBn_3$ fragment. A static structure accounting for the appearance of three different benzyl groups at low temperature is shown in Figure 2. This structure is similar to solid-state structures of **21** and **22** determined by single-crystal X-ray crystallography (vide infra).

As mentioned earlier, the major motivation for the preparation and investigation of complexes with the cyclohex-2-enylidene backbone was to identify complexes with high thermal stability. With a sample of **21** in hand, it was finally possible to answer the question about its thermal stability. A solution of **21** in toluene-d_8 was heated in the NMR probe to 89 °C for 42 h. To our delight, the NMR spectra showed very little (less than 4%) decomposition, indicating the very high thermal stability of **21**. This result stands in sharp contrast to imino-amido complexes, which undergo complete decomposition under the same conditions. The high thermal stability of **21** indicates that either its double-bond isomer is higher in energy and/or the pathway to reach the double-bond isomer of **21** is not accessible at this temperature. The calculated ground-state energy difference between **21**

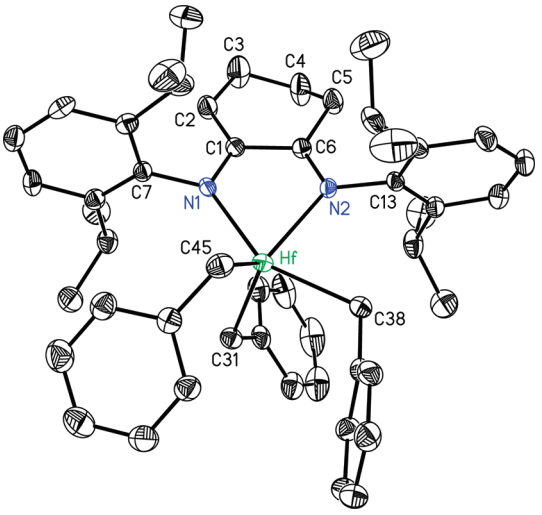

Figure 3. Molecular structure of **15**. Hydrogen atoms are omitted for clarity. Thermal ellipsoids are shown at the 40% probability level. Selected bond lengths (Å) and angle (deg): Hf−N1 = 2.164(3), Hf−N2 = 2.318(3), C1−N1 = 1.384(4), C6−N2 = 1.306(4), C1−C2 = 1.364(4), C5−C6 = 1.497(4); N2−Hf−N1 = 70.99(9).

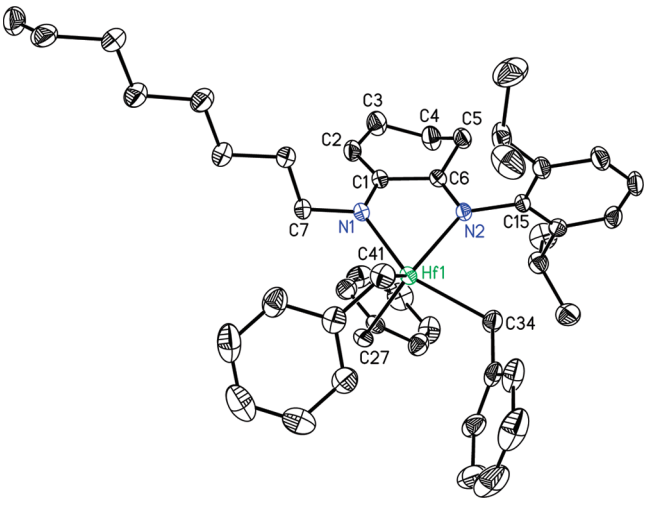

Figure 4. Molecular structure of **19**. Hydrogen atoms are omitted for clarity. Thermal ellipsoids are shown at the 40% probability level. Selected bond lengths (Å) and angle (deg): Hf−N1 = 2.079(2), Hf−N2 = 2.345(2), C1−N1 = 1.386(2), C6−N2 = 1.298(2), C1−C2 = 1.350(3), C5−C6 = 1.501(3); N2−Hf−N1 = 69.86(5).

and its isomer with the C═C and C═N double bonds transposed is only 1.0 kcal favoring **21**, whereas for the Zr analogue, the C═C/C═N bond isomer is more stable by 0.5 kcal than **22**. These calculations suggest that the high stability of **21** can be attributed to the lack of a kinetic pathway to access its double-bond isomer.

Single-Crystal X-ray Structures. The molecular structures of **15**, **19**, **21**, and **22** are shown in Figures 3−6, respectively, and selected bond lengths and angles are presented in Table 1. Metric parameters obtained for **15**, **19**, **21**, and **22** clearly confirm the identity of individual isomers originally established by NOESY experiments. For example, the C1−C2 bond length of 1.350(3) Å in **19** clearly indicates the presence of the double bond in the cyclohex-2-enylidene fragment bonded to the *N*-*n*-octyl

dx.doi.org/10.1021/om101207a |*Organometallics* 2011, 30, 1695–1709

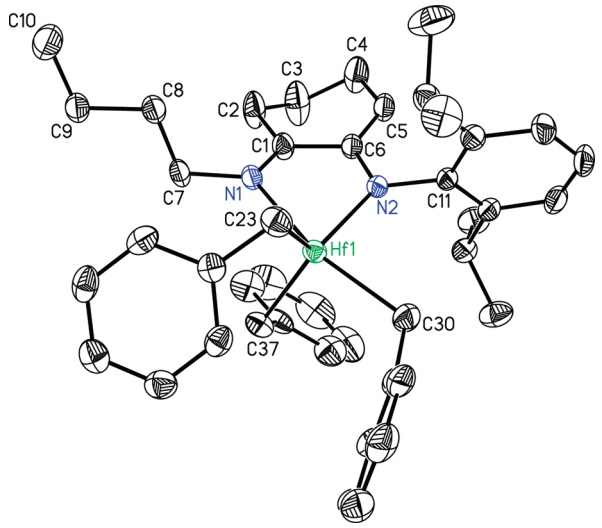

Figure 5. Molecular structure of **21**. Hydrogen atoms are omitted for clarity. Thermal ellipsoids are shown at the 40% probability level. Selected bond lengths (Å) and angle (deg): Hf−N1 = 2.164(3), Hf−N2 = 2.318(3), C1−N1 = 1.384(4), C6−N2 = 1.306(4), C1−C2 = 1.364(4), C5−C6 = 1.497(4); N2−Hf−N1 = 70.99(9).

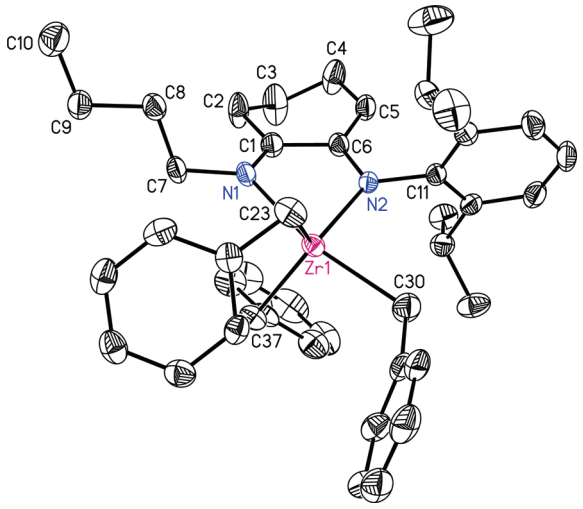

Figure 6. Molecular structure of **22**. Hydrogen atoms are omitted for clarity. Thermal ellipsoids are shown at the 40% probability level. Selected bond lengths (Å) and angles (deg): Zr−N1 = 2.332(3), Zr−N2 = 2.132(2), C1−N1 = 1.290(3), C6−N2 = 1.399(3), C1−C2 = 1.508(3), C5−C6 = 1.349(3); N2−Zr−N1 = 71.21(6).

fragment. The difference between the Hf−N(imino) and Hf−N(enamido) bond lengths in **15** (0.154 Å) is significantly smaller than that found in the imino-amido analogue **2** (0.283 Å). An analogous trend is observed between imino-enamido derivatives **19** and **21** and their imino-amido counterparts **6** and **5**, respectively. Additionally, the differences between C−N(imino) and C−N(enamido) bond lengths for **15**, **19**, **21**, and **22** are 0.078, 0.088, 0.113, and 0.109 Å, respectively, which are smaller than the differences found in **5** (0.227 Å) and **6** (0.163 Å). All this information indicates that the bonding in the five-membered metallacyclic rings in **15**, **19**, **21**, and **22** complexes is more symmetric than in the case of the imino-amido complexes. All benzyl groups are bonded in an η^1 fashion in these complexes.

Polymerization Results. New precatalysts were evaluated in ethylene/1-octene copolymerization reactions conducted in a 2 L batch reactor at both 120 and 150 °C. They were activated with 1.2 equiv (relative to precatalyst) of $[HNMe(C_{18}H_{37})_2][B(C_6F_5)_4]$ activator. All polymerization reactions were conducted in the presence of 10 mmol of hydrogen. Complex **15** was evaluated in comparison to the structurally similar imino-amido complex **2** (Table 2). The activity of **15** was 27.7 kg of polymer/mmol of catalyst, which is about 70% of that of **2**. Complex **15** gave polymers with slightly higher 1-octene incorporation levels, as shown by IR and polymer melting points (117.5 °C for **15** vs 121.3 °C for **2**). Interestingly, the molecular weight of ethylene/1-octene copolymer produced by **15** (M_w = 1002 kDa) was 3.5 times higher than that of **2** (M_w = 275 kDa). The activity of **21** (120 kg of polymer/mmol of catalyst), a direct analogue of **3**, was found to be about 1.5 times higher than that of **3**. Complex **21** resulted in a higher 1-octene incorporation rate than **3** (8.7 mol % 1-octene for **21** vs 5.5 mol % 1-octene for **3**). The polymer melting point as determined by DSC is in agreement with the IR measurements (74 °C for **21** vs 98 °C for **3**). Most significantly, the M_w value of polymer prepared by **21** was about 3.5 times higher than that of **3** (1037 kDa vs 283 kDa, runs 3 and 5). The ultrahigh molecular weights obtained for **15** and **21** are 20 times higher than that produced by the CGC complex, $\{(\eta^5\text{-}C_5Me_4)(SiMe_2\text{-}N\text{-}t\text{-}Bu)\}TiMe_2$, under the same conditions. Molecular weight capability is one of the most important characteristics of polyolefin catalysts, as it allows for the preparation of a larger array of products under various process conditions. It is simple to reduce the molecular weight of polyolefins to a desired level by the introduction of hydrogen during polymerization reactions, but it is much harder to increase the polymer's molecular weight for catalysts which undergo frequent termination events.[39] Complex **19** with its C═C and C═N double bonds transposed as compared to **21** was not very active (21 kg of polymer/mmol of catalyst) and gave a polymer with significantly reduced 1-octene content compared to that of **21** (3.7 mol % octene vs 8.7 mol % octene). The molecular weight of the copolymer produced by **19** was higher (M_w = 509 kDa) than that of **3** (M_w = 283 kDa) but lower than that made by **21**. Performance differences between **19** and **21** mirror those observed within the imino-amido catalyst family (**5a** vs **5b**).[6] The polymerization activity of complex **22**, the Zr analogue of **21**, was lower by 33% than that of **21** and was almost identical with that of **3**. 1-Octene incorporation is lower for **22** than for **21**, a trend also observed in related imino-amido complexes. The molecular weight of polymer prepared by **22** is lower than that of its Hf analogue **21** but higher than that of **3**. The catalytic performance of complex **21** at 150 °C (run 8) was 50% lower than at 120 °C, but it was still 3 times higher than that of **3** (run 9), due to an even steeper decline in activity (75%) for the latter. The molecular weight and 1-octene incorporation are significantly higher for **21** (M_w = 386 kDa, 7.0 mol % octene) than for **3** (M_w = 114 kDa, 4.4 mol % octene).

These data indicate that cyclohex-2-enylidene-bridged imino-enamido complexes have intrinsically higher molecular weight capabilities than the analogous trimethylethylidine-bridged imino-amido complexes. This phenomenon is seen in both the DIP-DIP (**15** vs **2**) and DIP-alkyl (**21** vs **3**) series of complexes. To gain insight into why imino-enamido catalysts lead to higher molecular weight polymers, end group analysis was performed by ^{1}H NMR spectroscopy on polymers prepared at 150 °C (runs 8 and 9, Figure 7). End group analysis allows for evaluating the identity and concentration of individual unsaturated functional groups resulting from chain termination events. The higher the

Table 1. Bond Lengths (Å) and Angles (deg) for Complexes 15, 19, 21, and 22, as Well as the Previously Reported 2 and 5a,b

bond length/angle	15	2[5]	19	21	22	5a[6]	5b[6]
Hf(Zr)−N1	2.164(3)	2.093(3)	2.079(2)	2.313(2)	2.332(2)	2.301(3)	2.030(4)
Hf(Zr)−N2	2.318(3)	2.376(3)	2.345(2)	2.100(2)	2.132(2)	2.074(3)	2.380(4)
Hf(Zr)−Bn1	2.233(3)	2.208(5)	2.247(2)	2.243(2)	2.266(2)	2.288(3)	2.291(5)
Hf(Zr)−Bn2	2.286(3)	2.221(5)	2.289(2)	2.288(2)	2.303(3)	2.259(3)	2.272(5)
Hf(Zr)−Bn3	2.222(3)	2.225(6)	2.235(2)	2.266(2)	2.286(2)	2.253(3)	2.242(5)
C1−C2	1.364(4)	1.518(6)	1.350(3)	1.498(3)	1.508(3)	1.509(5)	1.515(6)
C2−C3	1.475(5)		1.503(3)	1.523(4)	1.517(4)		
C3−C4	1.505(5)		1.517(3)	1.518(4)	1.517(4)		
C4−C5	1.497(5)		1.530(3)	1.491(3)	1.487(3)		
C5−C6	1.497(4)	1.552(7)	1.501(3)	1.347(3)	1.349(3)	1.539(5)	1.509(6)
C1−C6	1.470(4)	1.433(8)	1.462(2)	1.459(3)	1.460(3)	1.508(4)	1.515(6)
N1−C1	1.384(4)	1.314(6)	1.386(2)	1.290(3)	1.290(3)	1.270(5)	1.454(6)
N1−C7	1.452(4)	1.448(6)	1.471(2)	1.486(3)	1.478(3)	1.489(4)	1.475(5)
N2−C6	1.306(4)	1.495(5)	1.298(2)	1.403(2)	1.399(3)	1.497(4)	1.291(6)
N1−Hf(Zr)−N2	70.99(9)	69.99(13)	69.86(5)	72.03(6)	71.21(6)	72.6(1)	68.9(1)

Table 2. Polymerization Data for Complexes 2, 3, 15, 19, 21, 22, and CGC[a]

run	cat. (amt (μmol))	temp (°C)	amt of DEZ (μmol)	polymer yield (g)	cat. activity[b]	$10^{-3}M_w$*/PDI	T_m (°C)	octene content (mol %)
1	**2** (0.7)	120		26.7	38 100	275/2.3	121.3	2.4
2	**15** (0.7)	120		19.4	27 700	1002/3.1	117.5	5.4
3	**3** (0.7)	120		58.7	83 900	283/2.4	96.9	5.5
4	**19** (0.7)	120		14.7	21 000	506/1.8	104.7	3.4
5	**21** (0.4)	120		48.1	120 300	1037/2.4	76.0	8.7
6	**22** (0.4)	120		32.0	80 000	509/2.8	91.9	7.2
7	**CGC** (0.2)	120		39.1	195 500	47/2.3	58	14.8
8	**3** (1.0)	150		20.2	20 200	114/2.6	104.5	4.4
9	**21** (0.4)	150		24.7	61 800	386/2.4	79.8	7.0
10	**3** (0.7)	120	0	63.5	90 700	280/2.5	99.5	5.0
11	**3** (0.7)	120	140	72.2	103 100	199/1.9	102.3	5.0
12	**3** (0.7)	120	350	81.3	116 100	150/3.2	102.8	5.0
13	**21** (0.2)	120	0	31.9	159 500	1100/2.4	80	7.0
14	**21** (0.2)	120	40	21.9	109 500	499/1.9	89.7	6.0
15	**21** (0.2)	120	100	27.7	138 500	309/2.1	88.9	5.6

[a] Polymerization conditions: 533 mL of Isopar-E; 250 g of 1-octene; ethylene pressure 460 psi; hydrogen 10 mmol; pre-catalyst:activator = 1:1.2; activator $[HNMe(C_{18}H_{37})_2][B(C_6F_5)_4]$; 1:10 MMAO; reaction time 10 min. CGC = $\{(\eta^5\text{-}C_5Me_4)(SiMe_2\text{-}N\text{-}t\text{-}Bu)\}TiMe_2$. [b] Activity in units of g of polymer/mmol of catalyst.

native molecular weight a polymer exhibits, the lower the concentration of unsaturated polymer end groups measured (relative to polymer backbone). The total unsaturation found in polymers produced by **21** was 2.3 times lower than that in **3**, which is consistent with the molecular weight data.[40] The level of vinyl groups, which is a result of β-hydrogen elimination/chain transfer to monomer following a last inserted ethylene is virtually the same for both polymers (**21** and **3**), but the level of *cis*-/*trans*-vinylene (product of elimination after a 2,1-insertion of 1-octene) and vinylidene (product of elimination after a 1,2-insertion of 1-octene) groups is 4.1 and 3.0 times higher, respectively, for **3**. This analysis clearly indicates that the main reason for the higher molecular weight capability of **21** compared to that of **3** is the higher barrier of β-hydride elimination/chain transfer to monomer after 2,1- and 1,2-inserted 1-octene.

Since imino-amido complexes **2** and **3** were shown to produce olefin block copolymers (OBC),[5] it was of interest to us to determine if imino-enamido complexes such as **21** are capable of undergoing effective chain transfer reactions with diethylzinc (DEZ) during polymerization. The addition of 200 and 500 equiv of DEZ (relative to **21**) during polymerization resulted in a significant reduction of M_w from 1100 kDa (no DEZ) to 499 and 309 kDa, respectively. This represents a 72% decrease of M_w for a run with 500 equiv of DEZ. For **3**, the addition of 200 or 500 equiv of DEZ during polymerization resulted in a reduction in M_w from 280 kDa (no DEZ) to 199 and 150 kDa, respectively. Complex **21**, with its intermediate 1-octene incorporation, can be used to prepare either the soft or hard segment of OBCs, depending on the characteristics of the partnering catalyst and the design of the OBC.

CONCLUSIONS

Theoretical calculations revealed interesting trends of stability within cyclic and acyclic bis-imines and imine-enamines. Five- and six-membered-ring imine-enamines are considerably more stable

dx.doi.org/10.1021/om101207a |*Organometallics* 2011, 30, 1695–1709

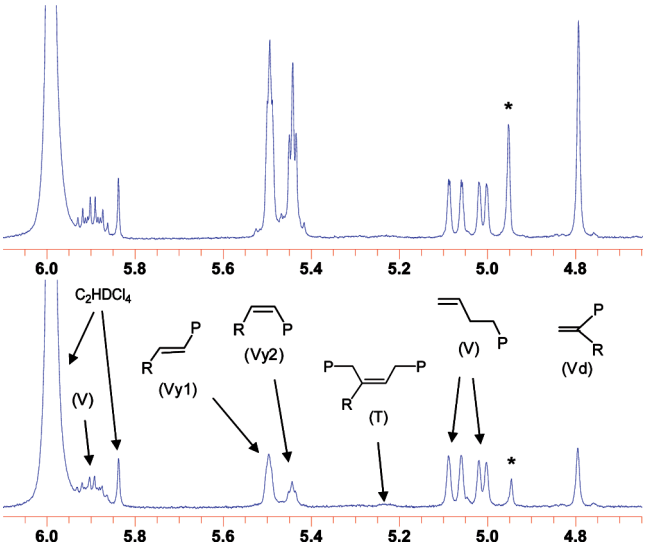

Figure 7. Fragment of ^{1}H NMR spectra of ethylene/1-octene copolymers obtained at 150 °C for **3** (run 8, top spectrum) and **21** (run 9, bottom spectrum). The asterisk designates an impurity from the antioxidant package.

than their corresponding bis-imines, due to favorable hydrogen bonding in imine-enamines and unfavorable lone-pair−lone-pair repulsions or steric interactions that exist in bis-imines. On the other hand, the lowest energy tautomer of the four- and seven-membered rings as well as the acyclic structures is the bis-imine. New imino-enamido complexes containing cyclohex-2-enylidene backbones were prepared in four steps, starting from the commercially available compound 1,2-cyclohexanedione. The last step in the ligand synthesis, imine formation, was the most challenging due to the unexpected ligand isomerization under acidic conditions. This difficulty was overcome by employing a Ti-imido reagent to introduce the imine functionality. As hoped, the imino-enamido complexes (e.g., **21**) bearing alkyl and aryl substituents on the imido and enamido nitrogen atoms, respectively, are thermally stable at 90 °C for many hours. This high thermal stability is in sharp contrast to that observed in analogous imino-amido complexes, which undergo a facile 1,2-Me shift at this temperature, producing isomeric complexes exhibiting poor polymerization characteristics. An ethylene/1-octene copolymerization study conducted at 120 °C demonstrated that the imino-enamido hafnium complex **21** has an activity 50% higher than that of the analogous imino-amido complex **3** and, more significantly, it produces polymers with higher molecular weight (M_w of 1037 kDa vs 283 kDa) and higher 1-octene content (8.0 vs 5.0 mol %) than for **3**. To a great extent, the molecular weight capability of a catalyst determines what type of polyolefin can be produced under given reactor conditions and is often a limiting factor for many catalysts. The ultrahigh-molecular-weight capability discovered for **15** and **21** is of importance, as catalysts capable of producing very high molecular weight polyolefins can be utilized at very high reactor temperatures, which is advantageous in the solution process. This very high molecular weight capability of **21** is a result of higher barriers for β-hydride elimination/chain transfer to monomer following 1-octene insertion as compared to the analogous imino-amido complex **3**, as shown by end group analysis. A polymerization study with **21** conducted in the presence of diethylzinc resulted in a sharp decrease of polymer molecular weight (from 1100 kDa to 309 kDa), indicating a very effective chain transfer reaction. The high thermal stability of new imino-amido complexes, coupled with their very good activity and ultrahigh-molecular-weight capability, makes them good candidates for the high-temperature synthesis of block and random ethylene/α-olefin copolymers.

Imino-enamido ligands are highly modular in nature, and various modifications to ligand structure should be possible via substitution variation on the imine and enamine nitrogen atoms and alterations to the ligand backbone. It is likely that even better performing imino-enamido catalysts can be identified via a comprehensive structure−reactivity study. On the mechanistic side, one wonders about the polymerization mechanism in these systems, since there are two alkyl groups remaining following precatalyst activation which might lead potentially to two polymeryl chains growing simultaneously at the metal center. These topics will be the subject of future reports.

EXPERIMENTAL SECTION

General Considerations. All solvents and reagents were obtained from commercial sources and used as received unless otherwise noted. Toluene, hexanes, CH_2Cl_2, and C_6D_6 were dried and degassed according to published procedures. NMR spectra were recorded on Varian Mercury-Vx-300 and VNMRS-500 spectrometers. ^{1}H NMR data are reported as follows: chemical shift (multiplicity (br = broad, s = singlet, d = doublet, t = triplet, q = quartet, p = pentet, and m = multiplet), integration, and assignment). Chemical shifts for ^{1}H NMR data are reported in ppm downfield from internal tetramethylsilane (TMS, δ scale) using residual protons in the deuterated solvent (C_6D_6, 7.15 ppm; toluene-d_8, 2.09 ppm) as references. ^{13}C NMR data were determined with ^{1}H decoupling, and the chemical shifts are reported in ppm vs tetramethylsilane (C_6D_6, 128 ppm; toluene-d_8, 20.4 ppm). Elemental analyses were performed at Midwest Microlab, LLC.

Preparation of *N*-[2-[[2,6-Bis(1-methylethyl)phenyl]amino]-2-cyclohexen-1-ylidene]-2,6-bis(1-methylethyl)benzenamine (9). This synthesis is based on a literature procedure.[11a] 1,2-Cyclohexanedione (2.062 g, 18.39 mmol) and 2,6-diisopropylaniline (6.52 g, 36.78 mmol) were dissolved in 70 mL of methanol. To this solution was added 1 mL of formic acid, and the mixture was stirred for 3 days at room temperature. Precipitated white crystalline solid was collected on the frit, washed with methanol (2 × 15 mL), and dried under reduced pressure to give 4.101 g (51.8%) of product.

Preparation of [*N*-[2-[[2,6-Bis(1-methylethyl)phenyl]-amino-κ*N*]-2-cyclohexen-1-ylidene]-2,6-bis(1-methylethyl)benzenaminato-κ*N*]tris(phenylmethyl)hafnium (15). *N*-[2-[[2,6-Bis(1-methylethyl)phenyl]amino]-2-cyclohexen-1-ylidene]-2,6-bis(1-methylethyl)benzenamine (0.439 g, 1.0 mmol) and tetrabenzylhafnium (0.554 g, 1.0 mmol) were dissolved in 6 mL of C_6D_6. The solution was heated for 4 days at 76 °C. NMR showed complete conversion of tetrabenzylhafnium with a product to ligand ratio of 9:1. Solvent was removed under reduced pressure. The remaining residue was dissolved in 3 mL of toluene and filtered. To the filtrate was added 8 mL of hexane. Within minutes yellow crystals appeared. After standing at ambient temperature for 3 h, 10 mL of hexane was added and the solution was put into a freezer (−26 °C) overnight. The solvent was decanted, and the yellow crystals were washed with hexane (2 × 10 mL) and dried under reduced pressure to give 0.486 g (54.5%) of product. ^{1}H NMR (C_6D_6, 500 MHz, 30 °C): 7.25 (m, 3H, *i*-Pr$_2$-*Ph*), 7.11 (tm, 6H, $^3J_{H-H}$ = 7.5 Hz, *m*-CH$_2$*Ph*), 7.06 (m, 3H, *i*-Pr$_2$-*Ph*), 6.84 (m, 3H, $^3J_{H-H}$ = 7.5 Hz, *p*-CH$_2$*Ph*), 6.61 (d, 6H, $^3J_{H-H}$ = 7.5 Hz, *o*-CH$_2$*Ph*), 4.96 (t, 1H, $^3J_{H-H}$ = 5.0 Hz, H5), 3.51 (sept. 2H, $^3J_{H-H}$ = 7.0 Hz, C*H*(CH$_3$)$_2$), 2.74 (sept. 2H, $^3J_{H-H}$ = 7.0 Hz, C*H*(CH$_3$)$_2$), 2.11 (br s, 6H, Hf−C*H*$_2$Ph), 1.98 (t, 2H, $^3J_{H-H}$ = 6.5 Hz, H2), 1.81 (q, 2H, $^3J_{H-H}$ = 5.6 Hz,

H4), 1.25 (p, 2H, $^3J_{H-H}$ = 6.0 Hz, H3), 1.22 (d, 6H, $^3J_{H-H}$ = 7.0 Hz, CH(CH_3)$_2$), 1.16 (d, 6H, $^3J_{H-H}$ = 6.5 Hz, CH(CH_3)$_2$), 1.14 (d, 6H, $^3J_{H-H}$ = 6.5 Hz, CH(CH_3)$_2$), 0.98 (d, 6H, $^3J_{H-H}$ = 7.0 Hz, CH-(CH_3)$_2$) ppm. ^{13}C{^{1}H} NMR (C_6D_6, 500 MHz, 30 °C): 181.90 (N=*C*), 150.03 (quat), 146.48 (quat, 145.91 (quat, 145.78 (quat, 144.12 (quat, 140.39 (quat), 128.57 (*m*-CH$_2$*Ph*), 128.26 (*o*-CH$_2$*Ph*), 128.00 (*i*-Pr$_2$-*Ph*), 126.89 (*i*-Pr$_2$-*Ph*), 125.07 (*i*-Pr$_2$-*Ph*), 124.87 (*i*-Pr$_2$-*Ph*), 122.45 (C5), 122.38 (*p*-CH$_2$*Ph*), 89.82 (Hf-*C*H$_2$Ph, $^1J_{C-H}$ = 116.9 Hz), 32.23 (C2), 29.15 (*C*H(CH$_3$)$_2$), 28.70 (*C*H(CH$_3$)$_2$), 26.93 (CH(*C*H$_3$)$_2$), 25.34 (C4), 25.10 (CH(*C*H$_3$)$_2$), 24.13 (CH(*C*H$_3$)$_2$), 23.80 (CH(*C*H$_3$)$_2$), 22.98 (C3) ppm. Anal. Calcd for $C_{51}H_{62}HfN_2$: C, 69.49; H, 7.09; N, 3.18. Found: C, 69.36; H, 6.96, N, 3.06.

Preparation of 2-(4-Morpholinyl)-2-cyclohexen-1-one (16). This synthesis is modified from a literature procedure.[32] A 500 mL round-bottom flask was equipped with a Dean−Stark trap, condenser, stir bar, and gas inlet (N_2 atmosphere). The flask was charged with of 1,2-cyclohexanedione (15.14 g, 135.00 mmol), morpholine (14.82 g, 170.10 mmol), and toluene (330 mL). The resulting yellow solution was heated at reflux for 5 h, resulting in the collection of about 3.0 mL of water in the Dean−Stark trap. The brown solution was decanted from thick oil and rinsed with toluene. The solution was concentrated under high vacuum to afford 23.33 g (95.34%) of a brown solid. ^{1}H NMR (C_6D_6, 300 MHz, 30 °C): δ 5.35 (t, 1H, ^3J = 4.6 Hz), 3.67−3.64 (m, 4H), 2.70−2.66 (m, 4H), 2.18−2.13 (m, 2H, H2), 1.87−1.81 (m, 2H, H4), 1.42 (quintet, 2H, ^3J = 6.4 Hz, H3) ppm. ^{13}C{^{1}H} NMR (C_6D_6, 75 MHz, 30 °C): δ 194.30, 147.03, 124.72, 67.32, 50.81, 40.49, 25.89, 23.63 ppm. GC/MS (CI) mass spectrum: m/z 182 (M + H).

Preparation of 2-[[2,6-Bis(1-methylethyl)phenyl]amino]-2-cyclohexen-1-one (17). A 250 mL three-necked round-bottom flask equipped with a condenser, gas inlet, and septum was placed under an N_2 atmosphere. The flask was charged with 2-(4-morpholinyl)-2-cyclohexen-1-one (7.0046 g, 38.65 mmol), toluene (80 mL), and 2,6-diisopropylaniline (6.8521 g, 38.65 mmol). To the yellow solution was added *p*-toluenesulfonic acid hydrate (7.3520 g, 38.65 mmol). The reaction mixture became very thick, due to heavy precipitate formation. The mixture was heated to 80 °C (oil bath temperature) and stirred for 2 h. After it was cooled to ambient temperature, the mixture was filtered. The filtrate was concentrated under vacuum to afford 10.09 g of a yellow solid. The solid was dissolved in hot hexanes (~30 mL) and filtered. After it was cooled to ambient temperature, the solution was placed in the freezer (−10 °C) overnight. The product was collected on a frit, washed with cold hexanes (2 × 6 mL), and dried under vacuum to give 4.0550 g of yellow solid. The filtrate was concentrated, and the resulting solid was recrystallized two more times, giving two additional crops (1.0785 and 0.6919 g). The combined yield was 5.8254 g (55.54%). ^{1}H NMR (C_6D_6, 300 MHz): δ 7.17−7.06 (m, 3H), 6.00 (broad s, 1H), 4.95 (t, 1H, J = 4.7 Hz), 3.15 (septet, 2H, J = 6.9 Hz), 2.21−2.16 (m, 2H, H2), 1.75 (q, 2H, J = 5.5 Hz, H4), 1.41 (quintet, 2H, J = 6.3 Hz, H3), 1.10 (d, 12H, J = 6.9 Hz) ppm. ^{13}C{^{1}H} NMR (C_6D_6, 75 MHz): δ 194.09, 147.17, 140.82, 135.90, 127.47, 124.04, 112.08, 38.15, 28.91, 24.53, 24.36, 24.04 ppm. GC/MS (CI) mass spectrum: m/z 272 (M + H). HRMS (ESI, (M + Na)$^+$): m/z calcd for $C_{18}H_{25}NONa$ 294.180, found 294.183.

Preparation of 2,6-Bis(1-methylethyl)-*N*-[(1*E*)-2-(octylamino)-2-cyclohexen-1-ylidene]benzenamine (18b). In the purge box, a 40.0 mL vial was charged with 2-[[2,6-bis(1-methylethyl)phenyl]amino]-2-cyclohexen-1-one (1.1128 g, 4.1003 mmol), toluene (20.0 mL), *n*-octylamine (0.680 mL, 4.1090 mmol), molecular sieves, and formic acid (0.16 mL, 4.1364 mmol). The mixture was shaken at 75 °C overnight. After it was cooled to ambient temperature, the solution was filtered to remove the molecular sieves and solvent was removed under reduced pressure to afford 1.5337 g of a thick yellow oil with some solid. The crude product was chromatographed using buffered silica gel and eluted with 1% Et_3N/0.5% ethyl acetate/98.5% hexanes to afford 0.9332 g (59.48%) of the product as a thick yellow oil. Note: TLC plates were buffered by treating with a solution of 5% triethylamine/95% hexanes for about 5 min and then allowed to dry. The silica gel for the column was also treated with a 5% triethylamine/95% hexanes solution and loaded in the column in that solution. ^{1}H NMR (C_6D_6, 500 MHz, 30 °C): δ 7.11−7.18 (m, 2H), 7.05−7.09 (m, 1H), 5.10 (t, 1H, ^3J = 5.3 Hz, N*H*), 5.04 (t, 1H, ^3J = 4.6 Hz, H2), 2.91 (q, 2H, ^3J = 7.0 Hz, H7), 2.87 (septet, 2H, ^3J = 7.0 Hz, C*H*(CH$_3$)$_2$), 2.17 (q, 2H, ^3J = 5.9 Hz, H3), 2.06 (pseudo t, 2H, ^3J = 6.5 Hz, H5), 1.54 (quintet, 2H, ^3J = 6.2 Hz, H4), 1.49 (quintet, 2H, ^3J = 7.2 Hz, H8), 1.19−1.32 (CH$_2$ overtone m, 10H), 1.19 (d, 6H, ^3J = 6.8 Hz, CH(CH_3)$_2$)), 1.15 (d, 6H, ^3J = 7.0 Hz, CH(CH_3)$_2$), 0.87 (t, 3H, ^3J = 7.0 Hz, H14) ppm. ^{13}C{^{1}H} NMR (C_6D_6, 125 MHz, 30 °C): δ 162.97, 146.38, 140.45, 136.59, 123.94, 123.34, 102.65, 43.62, 32.21, 29.83, 29.81, 29.70, 29.43, 28.56, 27.74, 24.94, 23.75, 23.64, 23.12, 23.05, 14.32 ppm. GC/MS (CI) mass spectrum: m/z 383 (M + H). HRMS (ESI, (M + H)$^+$): m/z calcd for $C_{26}H_{43}N_2$ 383.342, found 383.340.

Preparation of [2,6-Bis(1-methylethyl)-*N*-[(1*E*)-2-(octylamino-κ*N*)-2-cyclohexen-1-ylidene]benzenaminato-κ*N*]tris-(phenylmethyl)hafnium (19). In the glovebox, a vial was charged with 2,6-bis(1-methylethyl)-*N*-[(1*E*)-2-(octylamino)-2-cyclohexen-1-ylidene]benzenamine (0.3341 g, 0.8732 mmol), benzene (5.0 mL), and tetrabenzylhafnium (0.4741 g, 0.8731 mol). The solution became reddish brown. After about 5−10 min, ^{1}H NMR showed the desired complex and some $HfBn_4$ remaining. Therefore, a drop of the ligand was added. The mixture was stirred. The reaction mixture was concentrated under reduced pressure to afford 724 mg (99.5%) of the crude complex as a reddish sticky solid. The complex was further purified by recrystallization from hexanes at −40 °C to produce 346 mg of clean complex. ^{1}H NMR (toluene-d_8, 500 MHz, 30 °C): 7.20 (tm, 6H, $^3J_{H-H}$ = 8.0 Hz, *m*-CH$_2$*Ph*), 6.99−7.06 (m, 12H, *i*-Pr$_2$-*Ph* and *o*-CH$_2$*Ph*), 6.88 (tm, 3H, $^3J_{H-H}$ = 7.5 Hz, *p*-CH$_2$*Ph*), 5.13 (t, 1H, $^3J_{H-H}$ = 5.0 Hz, H2), 3.33 (m, 2H, H7), 2.35 (septet, 2H, $^3J_{H-H}$ = 6.5 Hz, C*H*(CH$_3$)$_2$), 2.12 (br s, 6H, Hf−CH_2Ph), 2.10 (q, 2H, $^3J_{H-H}$ = 5.6 Hz, H3), 1.89 (t, 2H, $^3J_{H-H}$ = 6.2 Hz, H5), 1.64 (m, 2H, H8), 1.27 (p, 2H, $^3J_{H-H}$ = 6.1 Hz, H4−determined by TOCSY1D), 1.27 (m, 10H, H9−H13), 1.15 (d, 6H, $^3J_{H-H}$ = 7.0 Hz, CH(CH_3)$_2$), 0.92 (d, 6H, $^3J_{H-H}$ = 6.5 Hz, CH(CH_3)$_2$), 0.91 (t, 3H, $^3J_{H-H}$ = 7.0 Hz, H10) ppm. ^{13}C{^{1}H} NMR (toluene-d_8, 125 MHz, 30 °C): 183.99 (N=*C*), 148.12 (quat), 146.08 (quat), 144.54 (quat), 139.94 (quat), 128.58 (*m*-CH$_2$*Ph*), 128.12 (*o*-CH$_2$*Ph*), 127.40 (*i*-Pr$_2$-*Ph*), 124.47 (*i*-Pr$_2$-*Ph*), 122.14 (*p*-CH$_2$*Ph*), 113.25 (C2), 85.23 (Hf-*C*H$_2$Ph, $^1J_{C-H}$ = 119.0 Hz), 45.72 (C7), 32.21, 31.80 (C5), 29.96, 29.89, 29.03 (*C*H(CH$_3$)$_2$), 28.09, 27.24 (C8), 25.33 (C3), 24.56 (CH(*C*H$_3$)$_2$), 24.19 (CH(*C*H$_3$)$_2$), 23.49, 23.04, 14.31 (C14). HSQCAD (toluene-d_8, 500 MHz): (7.20, 128.58), (6.99−7.06, 128.12/127.40/124.47), (6.88, 122.14), (5.13, 113.25), (3.33, 45.72), (2.35, 29.03), (2.12, 85.23), (2.10, 25.33), (1.89, 31.80), (1.64, 27.24), (1.28, 32.31/29.96/29.90/28.09/23.49/23.04), (1.15, 24.19), (0.92, 24.56), (0.91, 14.31) ppm. Anal. Calcd for $C_{47}H_{62}HfN_2$: C, 67.73; H, 7.50; N, 3.36. Found: C, 67.63; H, 7.47, N, 3.39.

Preparation of *n*-Butylamino-Titanium Reagent (Ti(N-*n*-Bu)$_2$)$_n$. $Ti(NMe_2)_4$ (26 g, 0.116 mol) was dissolved in 500 mL of toluene in a drybox in a Schlenk flask. The flask was taken into the hood. To this solution was added 68.8 mL (0.696 mol) of *n*-butylamine, which resulted in the formation of an orange solid. The mixture was heated at gentle reflux with a nitrogen sweep at the top of the condenser. The yellow solution became deep red within minutes after heating. After 6 h of reflux, the solution was cooled to room temperature and the solvent was removed under reduced pressure to give a deep red-black glassy solid. The product was transferred into the drybox for storage. A 23.29 g amount of product was obtained.

Preparation of *N*-[(6*E*)-6-(Butylimino)-1-cyclohexen-1-yl]-2,6-bis(1-methylethyl)benzenamine (20a). The reaction was carried out in a glovebox under an N_2 atmosphere. 2-[[2,6-Bis(1-

methylethyl)phenyl]amino]-2-cyclohexen-1-one (9.030 g, 33.273 mmol) was dissolved in toluene (400 mL) in a 1 L flask containing a stir bar. To the solution was added the titanium reagent (8.378 g, 24.905 mmol) followed by toluene (50 mL), giving a deep red-brown solution. The mixture was stirred for 2 days, resulting in the formation of copious amounts of brown precipitate. The mixture was filtered using a medium-porosity fritted-glass funnel. The brown solid was washed with toluene (4 × 50 mL). Solvent was removed under reduced pressure, leaving 9.005 g (82.9%) of the product as a yellow oil. ^{1}H NMR (C_6D_6, 500 MHz, 30 °C): δ 7.23−7.17 (m, 3H, *i*-Pr$_2$-*Ph*), 6.89 (s, 1H, NH), 4.78 (t, 1H, J = 4.6 Hz, H5), 3.39 (septet, 2H, ^3J = 6.9 Hz, C*H*(CH$_3$)$_2$), 3.26 (t, 2H, ^3J = 6.8 Hz, H7), 2.09 (pseudo t, 2H, ^3J = 6.6 Hz, H2), 1.96 (q, 2H, ^3J = 5.5 Hz, H4), 1.69 (pentet of multiplets, 2H, ^3J = 7.8 Hz, H8), 1.53 (quintet, 2H, ^3J = 6.5 Hz, H3), 1.44 (sextet of multiplets, 2H, ^3J = 7.0 Hz, H9), 1.22 (d, 12H, ^3J = 6.8 Hz, CH(C*H*$_3$)$_2$), 0.94 (t, 3H, ^3J = 7.3 Hz, H10) ppm. ^{13}C{^{1}H} NMR (C_6D_6, 125 MHz, 30 °C): δ 160.61, 147.38, 140.90, 137.89, 126.83, 123.80, 103.26, 49.84, 33.71, 28.69, 26.80, 24.23, 23.92, 23.39, 21.03, 14.21. HSQC (C_6D_6, 500 MHz): δ (7.23−7.17, 126.83/123.80), (4.78, 103.26), (3.39, 28.69), (3.26, 49.84), (2.09, 26.80), (1.96, 23.92), (1.69, 33.71), (1.52, 23.39), (1.44, 21.03), (1.22, 24.23), (0.94, 14.21) ppm. HRMS (ESI, (M + H)$^+$): m/z calcd for $C_{22}H_{35}N_2$ 327.277, found 327.280.

Preparation of (*E*)-2,6-Diisopropyl-*N*-[2-(butylamino)-cyclohex-2-enylidene]aniline (20b). *N*-[(6*E*)-6-(Butylimino)-1-cyclohexen-1-yl]-2,6-bis(1-methylethyl)benzenamine (108 mg) was dissolved in 587 mg of C_6D_6. To this solution was added 10 μL of 1.0 M HCl in diethyl ether, and the NMR tube was inserted into the NMR probe within 30 s. NMR spectra of this reaction mixture were followed over the course of 10 min. Isomerization was complete and quantitative within 10 min. ^{1}H NMR (C_6D_6, 500 MHz, 30 °C): 7.144 (d, 1H, $^3J_{H-H}$ = 8 Hz, *i*-Pr$_2$-*Ph*), 7.143 (d, 1H, $^3J_{H-H}$ = 7 Hz, *i*-Pr$_2$-*Ph*), 7.09 (dd, 1H, $^3J_{H-H}$ = 8.8 Hz, $^3J_{H-H}$ = 6.5 Hz, *i*-Pr$_2$-*Ph*), 5.11 (br s, 1H, N*H*), 5.04 (t, 1H, $^3J_{H-H}$ = 4 Hz, H2), 2.886 (t, 2H, $^3J_{H-H}$ = 7 Hz, H7), 2.881 (sept, 2H, $^3J_{H-H}$ = 6.9 Hz, C*H*(CH$_3$)$_2$), 2.16 (q, 2H, $^3J_{H-H}$ = 5.5 Hz, H3), 2.07 (m, 2H, H5), 1.53 (p, 2H, $^3J_{H-H}$ = 6.5 Hz, H3), 1.43 (pm, 2H, $^3J_{H-H}$ = 7.8 Hz, H8), 1.28 (sext-m, 2H, $^3J_{H-H}$ = 7.8 Hz, H9), 1.16 (d, 6H, $^3J_{H-H}$ = 6.9 Hz, CH(C*H*$_3$)$_2$), 1.13 (d, 6H, $^3J_{H-H}$ = 6.9 Hz, CH(C*H*$_3$)$_2$), 0.80 (t, 3H, $^3J_{H-H}$ = 7.4 Hz, H10) ppm. ^{13}C{^{1}H} NMR (C_6D_6, 125 MHz, 30 °C): 163.00 (N=*C*), 146.39 (quat), 140.42 (quat), 136.63 (quat), 123.95 (*C*H), 123.37 (*C*H), 112.83 (C2), 43.35 (C7), 31.47 (C8), 29.82 (C5), 28.56 (*C*H(CH$_3$)$_2$), 24.89 (C3), 23.71 (C4), 23.60 (CH(*C*H$_3$)$_2$), 23.09 (CH(*C*H$_3$)$_2$), 20.76 (C9), 14.02 (C10) ppm.

Preparation of [*N*-[(6*E*)-6-(Butylimino-κN)-1-cyclohexen-1-yl]-2,6-bis(1-methylethyl)benzenaminato-κN]tris(phenylmethyl)hafnium (21). *N*-[(6*E*)-6-(Butylimino)-1-cyclohexen-1-yl]-2,6-bis(1-methylethyl)benzenamine (0.3005 g, 0.92 mmol) and tetrabenzylhafnium (0.4997 mmol) were dissolved in toluene (6 mL) at room temperature, giving a light red solution. After this solution was stirred overnight (yellow solution), solvent was removed under reduced pressure, giving a highly crystalline yellow solid. The residue was dissolved in toluene (2 mL), followed by addition of hexane (8 mL). The solution was filtered and allowed to stand overnight at ambient temperature, resulting in the formation of large yellow crystals. The mother liquor was decanted, and the large yellow crystals were washed with cold hexane (5 mL) and dried under reduced pressure to give 331 mg of product. The mother liquor and hexane wash were combined and put into a freezer (−20 °C) overnight. The solvent was decanted and the resulting yellow crystals were washed with cold hexane (2 × 2 mL) and dried under reduced pressure to give 211 mg of product. Combined yield: 0.542 mg, 75.8%. ^{1}H NMR (toluene-d_8, 500 MHz, 30 °C): 7.18 (s, 3H, *i*-Pr$_2$-*Ph*), 7.11 (tm, 6H, $^3J_{H-H}$ = 7.6 Hz, *m*-CH$_2$*Ph*), 6.81, (m, 9H, *o*-/*p*-CH$_2$*Ph*), 4.57 (t, 1H, $^3J_{H-H}$ = 5.0 Hz, H5), 3.24 (sept, 2H, $^3J_{H-H}$ = 6.6 Hz, C*H*(CH$_3$)$_2$), 2.80 (m, 2H, H7), 2.11 (br s, 6H, Hf-C*H*$_2$Ph), 1.89 (t, 2H, $^3J_{H-H}$ = 6.7 Hz, H2), 1.83 (q, 2H, $^3J_{H-H}$ = 5.6 Hz, H4), 1.31 (d, 6H, $^3J_{H-H}$ = 6.9 Hz, CH(C*H*$_3$)$_2$), 1.29 (p, 2H, $^3J_{H-H}$ = 6.3 Hz, H3), 1.17 (m, 2H, H8), 1.11 (d, 6H, $^3J_{H-H}$ = 6.9 Hz, CH(C*H*$_3$)$_2$), 1.06 (sext, 2H, $^3J_{H-H}$ = 7.4 Hz, H9), 0.77 (t, 3H, $^3J_{H-H}$ = 6.9 Hz, H10) ppm. ^{13}C{^{1}H} NMR (toluene-d_8, 125 MHz, 30 °C): 175.87 (N=*C*), 151.58 (quat), 146.07 (quat), 145.00 (quat), 144.71 (quat), 128.61 (*m*-CH$_2$*Ph*), 127.25 (CH$_2$*Ph*), 126.29 (*i*-Pr$_2$-*Ph*), 124.36 (*i*-Pr$_2$-*Ph*), 121.80 (CH$_2$*Ph*), 116.93 (C5), 85.07 (Hf-*C*H$_2$Ph, $^1J_{C-H}$ = 117.4 Hz), 49.50 (N-*C*H$_2$), 30.46 (C8), 28.61 (*C*H(CH$_3$)$_2$), 28.28 (C2), 26.30 (CH(*C*H$_3$)$_2$), 24.87 (C4), 24.36 (CH(*C*H$_3$)$_2$), 22.88 (C3), 20.91 (C9), 13.74 (*C*H$_3$). HSQC (toluene-d_8, 500 MHz, 30 °C): (7.11, 128.61), (6.80, 127.25), (7.18, 126.29), (7.18, 124.36), (6.82, 121.80), (4.57, 116.93), (2.11, 85.07), (2.80, 49.50), (1.17, 30.46), (3.24, 28.61), (1.89, 28.28), (1.11, 26.30), (1.83, 24.87), (1.31, 24.36), (1.29, 22.88), (1.06, 20.91), (0.77, 13.74) ppm. HRMS (ESI, (M − Bn)$^+$): m/z calcd for $C_{36}H_{47}N_2Hf$ 687.321, found 687.324. Anal. Calcd for $C_{43}H_{54}HfN_2$: C, 66.43; H, 7.00; N, 3.60. Found: C, 66.58; H, 6.89, N, 3.65.

Preparation of [*N*-[(6*E*)-6-(Butylimino-κN)-1-cyclohexen-1-yl]-2,6-bis(1-methylethyl)benzenaminato-κN]tris(phenylmethyl)zirconium (22). *N*-[(6*E*)-6-(Butylimino)-1-cyclohexen-1-yl]-2,6-bis(1-methylethyl)benzenamine (0.350 g, 1.07 mmol) and tetrabenzylzirconium (0.4885 g, 1.07 mmol) were dissolved in 3 mL of benzene at room temperature to give a light red solution. After the mixture was stirred for 1 h, ^{1}H NMR showed that the reaction had reached completion. To the reaction mixture was added 8 mL of hexane; the solution was filtered and put into a freezer (−45 °C) overnight. The solvent was decanted, and the resulting yellow crystals were washed with cold hexane (2 × 4 mL) and dried under reduced pressure to give 0.566 g (68.1%) of product. ^{1}H NMR (C_6D_6, 500 MHz, 30 °C): 7.22 (pseudotriplet, 3H, *i*-Pr$_2$-*Ph*), 7.12 (tm, 6H, $^3J_{H-H}$ = 7.8 Hz, *m*-CH$_2$*Ph*), 6.88 (tm, 3H, $^3J_{H-H}$ = 7.0 Hz, *p*-CH$_2$*Ph*), 6.88 (dm, 6H, $^3J_{H-H}$ = 8.0 Hz, *o*-CH$_2$*Ph*), 4.64 (t, 1H, $^3J_{H-H}$ = 5.0 Hz, H5), 3.30 (sept, 2H, $^3J_{H-H}$ = 7.0 Hz, C*H*(CH$_3$)$_2$), 2.83 (m, 2H, H7), 2.24 (br s, 6H, Hf−C*H*$_2$Ph), 1.95 (t, 2H, $^3J_{H-H}$ = 6.3 Hz, H2), 1.78 (q, 2H, $^3J_{H-H}$ = 5.8 Hz, H4), 1.32 (d, 6H, $^3J_{H-H}$ = 6.5 Hz, CH(C*H*$_3$)$_2$), 1.28 (p, 2H, $^3J_{H-H}$ = 6.5 Hz, H3), 1.21 (m, 2H, H8), 1.14 (d, 6H, $^3J_{H-H}$ = 6.5 Hz, CH(C*H*$_3$)$_2$), 1.05 (sext, 2H, $^3J_{H-H}$ = 7.5 Hz, H9), 0.73 (t, 3H, $^3J_{H-H}$ = 7.5 Hz, H10) ppm. ^{13}C{^{1}H} NMR (C_6D_6, 125 MHz, 30 °C): 175.42 (N=C), 151.91 (quat), 146.44 (quat), 145.93 (quat), 144.73 (quat), 129.35 (*m*-CH$_2$*Ph*), 127.44 (*o*-CH$_2$*Ph*), 126.30 (*i*-Pr$_2$-*Ph*), 124.57 (*i*-Pr$_2$-*Ph*), 122.30 (*p*-CH$_2$*Ph*), 115.83 (C5), 75.11 (Hf-*C*H$_2$Ph, $^1J_{C-H}$ = 123.2 Hz), 50.20 (N-*C*H$_2$), 30.60 (C8), 28.55 (*C*H(CH$_3$)$_2$), 28.30 (C2), 26.55 (CH(*C*H$_3$)$_2$), 25.06 (C4), 24.23 (CH(*C*H$_3$)$_2$), 22.92 (C3), 20.75 (C9), 13.72 (*C*H$_3$) ppm. Information about C−H coupling constants comes from the proton-coupled ^{13}C experiment. HSQC (toluene-d_8, 300 MHz; ^{1}H resonance in ppm, ^{13}C resonance in ppm): (7.12, 129.35), (6.88, 127.44), (7.22, 126.30), (7.22, 124.57), (6.88, 122.30), (4.64, 115.83), (2.24, 75.11), (2.83, 50.20), (1.21, 30.60), (3.30, 28.55), (1.95, 28.30), (1.14, 26.55), (1.78, 25.06), (1.32, 24.23), (1.28, 22.92), (1.05, 20.75), (0.73, 13.72). HRMS (ESI, (M − Bn)$^+$): m/z calcd for $C_{36}H_{47}N_2Zr$ 597.279, found 597.282. Anal. Calcd for $C_{43}H_{54}ZrN_2$: C, 74.84; H, 7.89; N, 4.06. Found: C, 74.60; H, 7.73, N, 4.28.

Ethylene/1-Octene Polymerization Procedures and Polymer Characterizations. *Ethylene/1-Octene Copolymerization.* A 2 L Parr reactor was used in the polymerizations. All feeds were passed through columns of alumina and Q-5 catalyst (available from Engelhard Chemicals Inc.) prior to introduction into the reactor. Procatalyst and cocatalyst (activator) solutions were handled in the glovebox. A stirred 2 L reactor was charged with about 533 g of mixed alkanes solvent and 250 g of 1-octene comonomer. Hydrogen was added as a molecular weight control agent by differential pressure expansion from a 75 mL addition tank at 300 psi (2070 kPa). The reactor contents were heated to the polymerization temperature of 120 or 150 °C and saturated with ethylene at 460 psig (3.4 MPa). Catalysts and cocatalysts, as dilute solutions in toluene, were mixed and transferred to a catalyst addition

tank and injected into the reactor. The polymerization conditions were maintained for 10 min with ethylene added on demand. Heat was continuously removed from the reaction vessel through an internal cooling coil. The resulting solution was removed from the reactor, quenched with isopropyl alcohol, and stabilized by addition of 10 mL of a toluene solution containing approximately 67 mg of a hindered phenol antioxidant (Irganox 1010 from Ciba Geigy Corp.) and 133 mg of a phosphorus stabilizer (Irgafos 168 from Ciba Geigy Corp.).

Between polymerization runs, a wash cycle was conducted in which 850 g of mixed alkanes was added to the reactor and the reactor was heated to 150 °C. The reactor was then emptied of the heated solvent immediately before beginning a new polymerization run.

Polymers were recovered by drying for about 12 h in a temperature-ramped vacuum oven with a final set point of 140 °C. Melting and crystallization temperatures of polymers were measured by differential scanning calorimetry (DSC 2910, TA Instruments, Inc.). Samples were first heated from room temperature to 180 at 10 °C/min. After being held at this temperature for 2−4 min, the samples were cooled to −40 °C at 10 °C/min, held for 2−4 min, and then heated to 160 °C. Weight average molecular weights (M_w) and polydispersity values (PDI) were determined by analysis on a Viscotek HT-350 gel permeation chromatograph (GPC) equipped with a low-angle/right-angle light scattering detector, a four-capillary inline viscometer, and a refractive index detector. The GPC utilized three (3) Polymer Laboratories PLgel 10 μm MIXED-B columns (300 × 7.5 mm) at a flow rate of 1.0 mL/min in 1,2,4-trichlorobenzene at either 145 or 160 °C. To determine 1-octene incorporation, 140 μL of each polymer solution was deposited onto a silica wafer, heated to 140 °C until the trichlorobenzene had evaporated, and analyzed using a Nicolet Nexus 670 FTIR with version 7.1 software equipped with an AutoPro auto sampler.

End Group Analysis. Samples were dissolved in 8 mm NMR tubes in a solvent mixture, tetrachloroethane-d_2/perchloroethylene (50/50 v/v), with concentrations of 0.10 g/1.8 mL. The tubes were then heated in a heating block set at 120 °C. The sample tubes were repeatedly vortexed and heated to achieve a homogeneously flowing fluid. The ^{1}H NMR spectra were taken on a Varian Inova 600 MHz spectrometer. The following acquisition parameters were used: 25 s relaxation delay, 1 s presaturation (satpwr 1) on backbone (CH_2) protons, 90° pulse of 7.25 μs, 128 scans. All measurements were taken without sample spinning at 110 ± 1 °C. The ^{1}H NMR spectra were referenced at 5.99 ppm for the peak of residual tetrachloroethane-d_1.

Computational Details. Calculations used the Gaussian03 program.[41] Geometry optimizations and energies on ligands were done using two methods: (i) the hybrid density functional theory (DFT) method, B3LYP,[42] with the 6-311+G** basis set[43] and (ii) the G3MP2B3 level of theory.[44] For the metal−ligand complexes, structures were optimized with the B3LYP method and the LANL2TZ(F) basis set[45] on Hf/Zr along with 6-31G*(5d) on the remaining atoms. Single-point energies were done with the B3LYP/LANL2TZ(F)/6-311+G** method.

Structure Determinations of 10, 15, 19, 21, and 22. X-ray intensity data were collected on a Bruker SMART diffractometer using Mo Kα radiation (λ = 0.710 73 Å) and an APEXII CCD area detector. Raw data frames were read by the program SAINT[46] and integrated using 3D profiling algorithms. The resulting data were reduced to produce *hkl* reflections and their intensities and estimated standard deviations. The data were corrected for Lorentz and polarization effects, and numerical absorption corrections were applied on the basis of indexed and measured faces. The structure was solved and refined in SHELXTL6.1, using full-matrix least-squares refinement. The non-H atoms were refined with anisotropic thermal parameters, and all of the H atoms were calculated in idealized positions and refined riding on their parent atoms. The refinement was carried out using F^2 rather than F values. R1 was calculated to provide a reference to the conventional R value, but its function was not minimized.

Structure Determinations of 16 and 17. Crystals, mounted on a Mitegen Micromount, were automatically centered on a Bruker SMART X2S benchtop crystallographic system. Intensity measurements were performed using monochromated (doubly curved silicon crystal) Mo Kα radiation (0.710 73 Å) from a sealed microfocus tube. Generator settings were 50 kV and 1 mA. Data were acquired using three sets of ω scans at different ψ settings. APEX2 software was used for preliminary determination of the unit cell. Determinations of integrated intensities and unit cell refinement were performed using SAINT. Data were corrected for absorption effects with SADABS using the multiscan technique. The structures were solved with XS, and subsequent structure refinements were performed with XL.

■ ASSOCIATED CONTENT

Supporting Information. Tables with total energies for all computed structures, NMR spectra, X-ray data including CIF files, and a Mol file containing *xyz* data for all computed structures. This material is available free of charge via the Internet at http://pubs.acs.org.

■ AUTHOR INFORMATION

Corresponding Author

*To whom correspondence should be addressed. E-mail: jklosin@dow.com.

■ ACKNOWLEDGMENT

We thank Francis Timmers for help with cover art design.

■ REFERENCES

(1) (a) Britovsek, G. J. P.; Gibson, V. C.; Wass, D. F. *Angew. Chem., Int. Ed.* **1999**, *38*, 428–447. (b) Gibson, V. C.; Spitzmesser, S. K. *Chem. Rev.* **2003**, *103*, 283–316. (c) Makio, H.; Kashiwa, N.; Fujita, T. *Adv. Synth. Catal.* **2002**, *344*, 477–493. (d) Park, S.; Han, Y.; Kim, S. K.; Lee, J.; Kim, H. K.; Do, Y. *J. Organomet. Chem.* **2004**, *689*, 4263–4276.

(2) (a) Ittel, S. D.; Johnson, L. K.; Brookhart, M. *Chem. Rev.* **2000**, *100*, 1169–1203. (b) Tian, J.; Hustad, P. D.; Coates, G. W. *J. Am. Chem. Soc.* **2001**, *123*, 5134–5135. (c) Bollmann, A.; Blann, K.; Dixon, J. T.; Hess, F. M.; Killian, E.; Maumela, H.; McGuinness, D. S.; Morgan, D. H.; Neveling, A.; Otto, S.; Overett, M.; Slawin, A. M. Z.; Wasserscheid, P.; Kuhlmann, S. *J. Am. Chem. Soc.* **2004**, *126*, 14712–14713. (d) Boussie, T. R.; Diamond, G. M.; Goh, C.; Hall, K. A.; LaPointe, A. M.; Leclerc, M. K.; Murphy, V.; Shoemaker, J. A. W.; Turner, H.; Rosen, R. K.; Stevens, J. C.; Alfano, F.; Busico, V.; Cipullo, R.; Talarico, G. *Angew. Chem., Int. Ed.* **2006**, *45*, 3278–3283. (e) Arriola, D. J.; Carnahan, E. M.; Hustad, P. D.; Kuhlman, R. L.; Wenzel, T. T. *Science* **2006**, *312*, 714–719.

(3) (a) Klosin, J.; Kruper, W. J.; Nickias, P. N.; Roof, G. R.; De Waele, P.; Abboud, K. A. *Organometallics* **2001**, *20*, 2663–2665. (b) Konze, W. V.; Vanderlende, D. D. Int. Pat. Appl. 2007136497, 2007. (c) Nabika, M.; Katayama, H.; Watanabe, T.; Kawamura-Kuribayashi, H.; Yanagi, K.; Imai, A. *Organometallics* **2009**, *28*, 3785–3792.

(4) De Waele, P.; Jazdzewski, B. A.; Klosin, J.; Murray, R. E.; Petersen, J. L.; Theriault, C. N.; Vosejpka, P. C. *Organometallics* **2007**, *26*, 3896–3899.

(5) Kuhlman, R. L.; Klosin, J. *Macromolecules* **2010**, *43*, 7903–7904.

(6) Froese, R. D.; Jazdzewski, B. A.; Klosin, J.; Kuhlman, R. L.; Theriault, C. N.; Welsh, D. M.; Abboud, K. A. *Organometallics* **2011**, *30*, 251–262.

(7) (a) Mashima, K.; Ohnishi, R.; Yamagata, T.; Tsurugi, H. *Chem. Lett.* **2007**, *36*, 1420–1421. (b) Tsurugi, H.; Ohnishi, R.; Kaneko, H.; Panda, T. K.; Mashima, K. *Organometallics* **2009**, *28*, 680–687. (c) Kaneko, H.; Tsurugi, H.; Panda, T. K.; Mashima, K. *Organometallics* **2010**, *29*, 3463–3466.

(8) (a) Murray, R. E. U.S. Patent 6,096,676, 2000. (b) Murray, R. E.; George, V. M.; Nowlin, D. L.; Schultz, C. C.; Petersen, J. L. *Polym. Prepr. (Am. Chem. Soc., Div. Polym. Chem.)* **2002**, *43*, 294–295. (c) Murray, R. E. Int. Pat. Appl. 2003051935, 2003.

(9) van Asselt, R.; Elsevier, C. J.; Smeets, W. J. J.; Spek, A. L.; Benedix, R. *Recl. Trav. Chim. Pays-Bas* **1994**, *113*, 88–98.

(10) Kiyotaka B.; Masatoshi, N.; Daisuke, F. JP Patent 10182679, 1998.

(11) (a) Johnson, L. K.; Bennett, A. M. A.; Ittel, S. D.; Wang, L.; Parthasarathy, A.; Hauptman, E.; Simpson, R. D.; Feldman, J.; Coughlin, E. B. Int. Pat. Appl. 9830609, 1998. (b) Gates, D. P.; Svejda, S. A.; Onate, E.; Killian, C. M.; Johnson, L. K.; White, P. S.; Brookhart, M. *Macromolecules* **2000**, *33*, 2320–2334.

(12) Lodochnikov, V. G.; Gryaznova, T. V.; Gryaznov, P. I.; Musin, R. Z.; Kibardin, A. M. *Russ. J. Gen. Chem.* **2001**, *71*, 437–442.

(13) Al-Omari, M.; Banert, K.; Hagedorn, M. *Angew. Chem., Int. Ed.* **2006**, *45*, 309–311.

(14) Kiesewetter, J.; Kaminsky, W. *Chem. Eur. J.* **2003**, *9*, 1750–1758.

(15) Pappalardo, D.; Tedesco, C.; Pellecchia, C. *Eur. J. Inorg. Chem.* **2002**, 621–628.

(16) Cationic, acyclic imido-enamido complexes of zirconium have been previously reported by the reaction of buta-1,3-diene-2,3-diamido complexes with strong Lewis acids: Kim, Y H.; Kim, T. H.; Kim, N. Y.; Cho, E. S.; Lee, B. Y.; Shin, D. M.; Chung, Y. K. *Organometallics* **2003**, *22*, 1503–1511.

(17) Kim, Y. H.; Kim, T. H.; Lee, B. Y.; Woodmansee, D.; Bu, X.; Bazan, G. C. *Organometallics* **2002**, *21*, 3082–3084.

(18) Figueroa, R.; Klosin, J. Int. Pat. Appl. 2010022228, 2010.

(19) The relative energies (kcal/mol) discussed in the text are enthalpies. DFT ground-state energies for *i*-Pr- and DIP-based derivatives for compounds shown in Scheme 4 are presented in the Supporting Information.

(20) Three-dimensional structures of all calculated compounds are included in the Supporting Information (MOL file format). MOL files can be read by many programs, including the Mercury program freely available at http://www.ccdc.cam.ac.uk/products/mercury/.

(21) There is one example of a structurally characterized six-membered-ring derivative that exists as a bis-imine rather than an imine-enamine. In this case, however, both imine nitrogen atoms bear an unsaturated group (3-pentene-2-thione) that stabilizes the bis-imine form via conjugation: Jensen, H. P.; Kristensen, B. S.; Mosbaek, H.; Søtofte, I. *Acta Chem. Scand.* **1978**, *A32*, 141–148.

(22) *N*-methyl mono-imines are calculated to be more stable than the corresponding enamines by 3.0 (five-membered), 1.6 (six-membered), and 0.3 kcal/mol (seven-membered).

(23) 1-Methylcycloalkenes are more stable than methylenecycloalkanes by 3.3 (five-membered ring), 7.2 (six-membered ring), and 2.3 kcal/mol (seven-membered ring).

(24) Smith, M. B.; March, J. *March's Advanced Organic Chemistry: Reactions, Mechanisms, and Structure*; Wiley: Hoboken, NJ, 2007; p 107.

(25) For crystal structures of acenaphthalene-based bis-imines with trans/trans configuration see:(a) Liu, H.-R.; Gomes, P. T.; Costa, S. I.; Duarte, M. T.; Branquinho, R.; Fernandes, A. C.; Chien, J. C. W.; Singh, R. P.; Marques, M. M. *J. Organomet. Chem.* **2005**, *690*, 1314–1323. (b) Coventry, D. N.; Batsanov, A. S.; Goeta, A. E.; Howard, J. A. K.; Marder, T. B. *Polyhedron* **2004**, *23*, 2789–2795. (c) Zou, H.; Hu, S.; Huang, H.; Zhu, F.; Wu, Q. *Eur. Polym. J.* **2007**, *43*, 3882–3891.

(26) For crystal structures of cyclic bis-imines with trans/cis configuration see: (a) Moore, J. A.; Vasudevan, K.; Hill, N. J.; Reeske, G.; Cowley, A. H. *Chem. Commun.* **2006**, 2913–2915. (b) Rosa, V.; Avilés, T.; Aullon, G.; Covelo, B.; Lodeiro, C. *Inorg. Chem.* **2008**, *47*, 7734–7744. (c) Schleis, T.; Heinemann, J.; Spaniol, T. P.; Mulhaupt, R.; Okuda, J. *Inorg. Chem. Commun.* **1998**, *1*, 431–434. (d) Fedushkin, I. L; Chudakova, V. N.; Skatova, A. A.; Khvoinova, N. M.; Kurskii, Y. A.; Glukhova, T. A.; Fukin, G. K.; Dechert, S.; Hummert, M.; Schumann, H. *Z. Anorg. Allg. Chem.* **2004**, *630*, 501–507. (e) Lentz, D. *Z. Naturforsch., B: Chem. Sci.* **1992**, *47*, 148–150. (f) Adams, C. J.; Anderson, K. M.; Bartlett, I. M.; Connelly, N. G.; Orpen, A. G.; Paget, T. J.; Phetmung, H.; Smith, D. W. *Dalton Trans.* **2001**, 1284–1292.

(27) The energy difference between trans/trans and trans/cis bis-imines based on acenaphthalene bearing smaller substituents on imine nitrogen atoms must be small, as both isomers are seen in solid-state structures. For acenaphthalene bis-imines with *o*-CF_3-Ph substituents on nitrogen atoms, both trans/trans and trans/cis isomers are observed in the unit cell.[26a]

(28) For examples of acyclic bis-imines with σ-trans conformation see:(a) Gerdes, G.; Chen, P. *Organometallics* **2003**, *22*, 2217–2225. (b) Ionkin, A. S.; Marshall, W. J. *Organometallics* **2004**, *23*, 3276–3283. (c) Gonsalvi, L.; Gaunt, J. A.; Adams, H.; Castro, A.; Sunley, G. J.; Haynes, A. *Organometallics* **2003**, *22*, 1047–1054. (d) Ionkin, A. S.; Marshall, W. J. *J. Organomet. Chem.* **2004**, *689*, 1057–1063.

(29) Amii, H.; Kohda, M.; Seo, M.; Uneyama, K. *Chem. Commun.* **2003**, 1752–1753. (b) Sadighi, J. P.; Henling, L. M.; Labinger, J. A.; Bercaw, J. E. *Tetrahedron Lett.* **2003**, *44*, 8073–8076. (c) Lersch, M.; Krivokapic, A.; Tilset, M. *Organometallics* **2007**, *26*, 1581–1587.

(30) The $^{13}C\{^1H\}$ NMR spectrum for the seven-membered-ring bis-imine[13] exhibits only one signal for the imine or methine carbons, but two carbon resonances are recorded for the *i*-Pr methyl groups. Two methyl groups and only one methine proton are also observed in the ^1H NMR spectrum. This indicates that the *i*-Pr methyl groups are diastereotopic, which implies a chiral environment. Bis-imine **13c** is chiral, and because of its cis/cis configuration, the barrier for interconversion between enantiomers is expected to be high. The bis-imine with a trans/trans configuration (**13a**) is also chiral in the ground state, but because of the significantly lower steric congestion between the imine nitrogen atoms, it would be expected to undergo fast interconversion between enantiomers at ambient temperature, resulting in the appearance of only one signal for the *i*-Pr methyl peak (C_{2v} symmetry in solution).

(31) Structures and energies of various cyclic 1,2-keto-enamines/1,2-keto-imines and 1,2-keto-enol/1,2-diketones are included in the Supporting Information.

(32) See the Supporting Information for NMR spectra.

(33) Ōhashi, M.; Takahashi, T.; Inoue, S.; Sato, K. *Bull. Chem. Soc. Jpn.* **1975**, *48*, 1892–1896.

(34) See the Supporting Information for details.

(35) (a) Polozov, G. I.; Tishchenko, I. G. *Vestn. Belorus. Un-ta, Ser. 2* **1986**, *1*, 67–69. (b) Dounay, A. B.; Overman, L. E.; Wrobleski, A. D. *J. Am. Chem. Soc.* **2005**, *127*, 10186–10187.

(36) (a) Carlson, R.; Nilsson, A. *Acta Chem. Scand.* **1984**, *B 38*, 49–53. (b) Armesto, D.; Bosch, P.; Gallego, M. G.; Martin, J. F.; Ortiz, M. J.; Pérez-Ossorio, R.; Ramos, A. *Org. Prep. Proced. Int.* **1987**, *19*, 181–186. (c) De Kimpe, N.; D'hondt, L.; Stanoeva, E. *Tetrahedron Lett.* **1991**, *32*, 3879–3882. (d) Carlson, R.; Larsson, U.; Hansson, L. *Acta Chem. Scand.* **1992**, *46*, 1211–1214. (e) Klosin, J. U.S. Patent 6,617,407, 2003.

(37) Bradley, D. C.; Torrible, E. G. *Can. J. Chem.* **1963**, *41*, 134–138.

(38) (a) Schleis, T.; Spaniol, T. P.; Okuda, J.; Heinemann, J.; Mülhaupt, R. *J. Organomet. Chem.* **1998**, *569*, 159–167. (b) Bianchini, C.; Giambastiani, G.; Rios, I. G.; Mantovani, G.; Meli, A.; Segarra, A. M. *Coord. Chem. Rev.* **2006**, *250*, 1391–1418.

(39) It is possible to increase M_w by decreasing the reactor temperature, but this is usually not a practical and economical solution.

(40) The ratio of molecular weights of polymers generated by **21** and **3** is 3.6, which is measurably higher than that obtained from end group analysis (2.3). This difference is most likely due to the slightly higher reactivity of **3** toward hydrogen compared to **21**.

(41) Frisch, M. J.; Trucks, G. W.; Schlegel, H. B.; Scuseria, G. E.; Robb, M. A.; Cheeseman, J. R.; Montgomery, Jr., J. A.; Vreven, T.; Kudin, K. N.; Burant, J. C.; Millam, J. M.; Iyengar, S. S.; Tomasi, J.; Barone, V.; Mennucci, B.; Cossi, M.; Scalmani, M. G.; Rega, N.; Petersson, G. A.; Nakatsuji, H.; Hada, H.; Ehara, M.; Toyota, M. K.; Fukuda, R.; Hasegawa, J.; Ishida, M.; Nakajima, T.; Honda, Y.; Kitao, O.; Nakai, H.; Klene, M.; Li, X.; Knox, J. E.; Hratchian, H. P.; Cross, J. B.; Adamo, C.; Jaramillo, J.; Gomperts, R.; Stratmann, R. E.; Yazyev, O.; Austin, A. J.; Cammi, R.; Pomelli, C.; Ochterski, J. W.; Ayala, P. Y.; Morokuma, K.; Voth, G. A.; Salvador, P.; Dannenberg, J. J.; Zakrzewski, V. G.; Dapprich, S.; Daniels, A. D.; Strain, M. C.; Farkas, O.; Malick, D. K.; Rabuck, A. D.; Raghavachari, K.; Foresman, J. B.; Ortiz, J. V.; Cui,

Q.; Baboul, A. G.; Clifford, S.; Cioslowski, J.; Stefanov, B. B.; Liu, G.; Liashenko, A.; Piskorz, P.; Komaromi, I.; Martin, R. L.; Fox, D. J.; Keith, T.; Al-Laham, M. A.; Peng, C. Y.; Nanayakkara, A.; Challacombe, M.; Gill, P. M. W.; Johnson, B.; Chen, W.; Wong, M. W.; Gonzalez, C.; Pople, J. A. *Gaussian 03, Revision C.02*; Gaussian, Inc., Wallingford, CT, 2004.

(42) (a) Becke, A. D. *J. Chem. Phys.* **1993**, *98*, 5648. (b) Lee, C.; Yang, W.; Parr, R. G. *Phys. Rev. B* **1988**, *37*, 785. (c) Miehlich, B.; Savin, A.; Stoll, H.; Preuss, H. *Chem. Phys. Lett.* **1989**, *157*, 200.

(43) (a) Ditchfield, R.; Hehre, W. J.; Pople, J. A. *J. Chem. Phys.* **1971**, *54*, 724. (b) Hehre, W. J.; Ditchfield, R.; Pople, J. A. *J. Chem. Phys.* **1972**, *56*, 2257. (c) Gordon, M. S. *Chem. Phys. Lett.* **1980**, *76*, 163.

(44) (a) Curtiss, L. A.; Redfern, P. C.; Raghavachari, K.; Rassolov, V.; Pople, J. A. *J. Chem. Phys.* **1999**, *110*, 4703. (b) Baboul, A. G.; Curtiss, L. A.; Redfern, P. C.; Raghavachari, K. *J. Chem. Phys.* **1999**, *110*, 7650.

(45) (a) Dunning, T. H., Jr.; Hay, P. J. In *Modern Theoretical Chemistry*; Schaefer, H. F., III, Ed.; Plenum: New York, 1976; Vol. 3, p 1. (b) Hay, P. J.; Wadt, W. R. *J. Chem. Phys.* **1985**, *82*, 270. (c) Wadt, W. R; Hay, P. J. *J. Chem. Phys.* **1985**, *82*, 284. (d) Hay, P. J.; Wadt, W. R. *J. Chem. Phys.* **1985**, *82*, 299. (e) Roy, L. E.; Hay, P. J.; Martin, R. L. *J. Chem. Theory Comput.* **2008**, *4*, 1029.

(46) Sheldrick, G. M. *SHELXTL6.1 Crystallographic Software Package*; Bruker AXS, Inc., Madison, WI, 2008.